SMART WATER DISPLACEMENT
AN ALTERNATIVE ENHANCED OIL RECOVERY TECHNIQUE

A THESIS SUBMITTED TO
THE GRADUATE SCHOOL OF NATURAL AND APPLIED SCIENCES
OF
MIDDLE EAST TECHNICAL UNIVERSITY

BY

CAN POLAT

IN PARTIAL FULFILLMENT OF THE REQUIREMENTS
FOR
THE DEGREE OF DOCTOR OF PHILOSOPHY
IN
PETROLEUM AND NATURAL GAS ENGINEERING

NOVEMBER 2015

Approval of the thesis:

SMART WATER DISPLACEMENT

AN ALTERNATIVE ENHANCED OIL RECOVERY TECHNIQUE

submitted by **CAN POLAT** in partial fulfillment of the requirements for the degree of **Doctor of Philosophy in Petroleum and Natural Gas Engineering, Middle East Technical University** by,

Prof. Dr. Gülbin Dural Ünver _____
Dean, Graduate School of **Natural and Applied Sciences**

Prof. Dr. Mustafa Verşan Kök _____
Head of Department, **Petroleum and Natural Gas Engineering**

Prof. Dr. Mahmut Parlaktuna _____
Supervisor, **Petroleum and Natural Gas Engineering Dept., METU**

Prof. Dr. Salih Saner _____
Co-Supervisor, **Petroleum and Natural Gas Engineering Dept., METU**

Examining Committee Members:

Prof. Dr. Ender Okandan _____
Petroleum and Natural Gas Engineering Dept., METU

Prof. Dr. Mahmut Parlaktuna _____
Petroleum and Natural Gas Engineering Dept., METU

Prof. Dr. Ahmet Tuğrul Başokur _____
Geophysical Engineering Dept., Ankara University

Assoc. Prof. Dr. Ömer İnanç Türeyen _____
Petroleum and Natural Gas Engineering Dept., Istanbul Technical University

Asst. Prof. Dr. Çağlar Sınayuç _____
Petroleum and Natural Gas Engineering Dept., METU

Date: 16.11.2015

I hereby declare that all information in this document has been obtained and presented in accordance with academic rules and ethical conduct. I also declare that, as required by these rules and conduct, I have fully cited and referenced all material and results that are not original to this work.

Name, Last name : Can POLAT

Signature :

ABSTRACT

SMART WATER DISPLACEMENT

AN ALTERNATIVE ENHANCED OIL RECOVERY TECHNIQUE

Polat, Can

Ph.D., Department of Petroleum and Natural Gas Engineering

Supervisor : Prof. Dr. Mahmut Parlaktuna

Co-Supervisor : Prof. Dr. Salih Saner

November 2015, 103 pages

The aim of this study is to investigate the effect of smart water displacement on oil recovery. The brine samples were prepared considering the characteristics of the samples proved to be effective in oil recovery. The effect of these brine samples on rock wettability was observed using Modified Flotation Test (MFT) procedure. The effect of changing brine salinity on interfacial tension between brine and oil samples was observed using interfacial tension meter and ring tensiometer. Liquids used in spontaneous imbibition and coreflooding experiments were determined considering the results of wettability and interfacial tension measurements. Flow was visualized

under video camera and computer tomography (CT) was applied during the coreflooding experiments.

The results indicate that using sulfate ion with divalent cations, Ca^{2+} and Mg^{2+} in low saline brine increases water wettability for carbonates and removing divalent cations from the brine samples increases water wettability for sandstones poor in clay content in comparison to wettability obtained with formation brine sample utilization. High water wettability can be achieved for carbonates even at low temperatures increasing the sulfate concentration. Improvement in spontaneous imbibition into the rock sample can be achieved decreasing the interfacial tension between brine oil using surfactant or decreasing the salinity of the brine sample, proved to be also effective in the core floooding experiment including flow visualization. In the core flooding experiment including the application of CT, it was observed that direct utilization of sulfated brine including divalent cations without injecting the high saline brine used to saturate the core sample previously resulted in more oil production.

Keywords: Smart Water, Enhanced Oil Recovery

ÖZ

AKILLI SU ÖTELEMESİ

ALTERNATİF GELİŞMİŞ PETROL KURTARIMI YÖNTEMİ

Polat, Can

Doktora, Petrol ve Doğal Gaz Mühendisliği Bölümü

Tez Yöneticisi : Prof. Dr. Mahmut Parlaktuna

Ortak Tez Yöneticisi : Prof. Dr. Salih Saner

Kasım 2015, 103 sayfa

Bu çalışmanın amacı akıllı su ötelemesinin petrol kurtarımına olan etkisini incelemektir. Su örnekleri petrol kurtarımında etkili olduğu kanıtlanan numulerin özellikleri dikkate alınarak hazırlanmıştır. Bu su örneklerinin kayaç ıslanırlığına olan etkisi modifiye edilmiş flotasyon test yöntemi kullanılarak gözlemlenmiştir. Su tuzluluğunu değiştirmenin petrol ve su arasındaki yüzey gerilimine olan etkisi tansiometrelerle gözlemlenmiştir. Doğal imbibisyon ve akış deneylerinde kullanılan sıvılar ıslanırlık ve yüzey gerilimi ölçümlerinden çıkan sonuçlar dikkate alınarak hazırlanmıştır. Akış video kamera ile görselleştirilmiş ve ayrıca akış deneyi sırasında bilgisayar tomografisi uygulanmıştır.

Sonuçlar, sülfat iyonunun iki değerlikli katyonlarla birlikte az tuzlu suda kullanılmasının karbonatların su ile olan ıslanırlığını ve ayrıca iki değerlikli katyonların tuzlu sudan çıkarılmasının kil miktarı az olan kumtaşının su ile olan ıslanırlığını formasyon suyu kullanılarak elde edilen ıslanırlıklara kıyasla artırdığını göstermiştir. Karbonat için yüksek su ıslanırlığı sülfat konsantrasyonu artırarak düşük sıcaklıkta da elde edilmiştir. Doğal imbibisyondaki gelişim su ve pertol arasındaki yüzey geriliminin görselleştirilen akış deneyinde de etkili olduğu kanıtlanan yüzey etkinleştirici kullanma ve suyun tuzluluğunu azaltma işlemleri ile düşürülmesiyle elde edilmiştir. Bilgisayar tomografi kullanımını içeren akış deneyinde, karot örneğini doyurmakta kullanılan yüksek tuzlu suyun önceden enjekte edilmeyerek iki değerlikli katyonları içeren sülfatlı suyun direkt kullanılmasının daha çok petrol üretimine yol açtığı gözlemlenmiştir.

Anahtar Kelimeler: Akıllı Su, Gelişmiş Petrol Kurtarımı

ACKNOWLEDGEMENTS

I would like to thank to Prof. Dr. Mahmut Parlaktuna and Prof. Dr. Salih Saner for their guidance, advice and support throughout the thesis study.

I would also like to thank to Murat Akın, Sevtaç Bülbül and Naci Doğru for their assistance throughout the experimental study.

Measurement of interfacial was performed in Turkish Petroleum Research Center. I would like to thank to Artuğ Türkmenoğlu and Cansu Ulak for their help during the measurement.

The oil samples were analyzed in METU Petroleum Research Center. I would like to thank to employees of METU Petroleum Research Center for their contribution during the thesis study.

CT scans were performed in core tomography laboratory of Petroleum Research Center of METU. I would like to thank to Hasan Turmuş for his contribution during the measurement.

TABLE OF CONTENTS

ABSTRACT..... v
ÖZ..... vii
ACKNOWLEDGEMENTS..... ix
TABLE OF CONTENTS..... x
LIST OF TABLES..... xiii
LIST OF FIGURES..... xiv
CHAPTERS
1. INTRODUCTION..... 1
2. LITERATURE REVIEW..... 5
2.1. Wettability and Smart Water..... 5
2.2. Wettability Alteration..... 6
2.3. Smart Water in Carbonates..... 7
2.4. Smart Water in Sandstones..... 9
2.5. Factors Affecting the Efficiency of Smart Water..... 10
2.5.1. Initial Wettability..... 10
2.5.1.1. Wettability Alteration..... 10
2.5.1.2. Mechanisms Behind Wettability Alteration..... 11
2.5.1.3. Effect of Oil Properties on Wettability Alteration..... 12
2.5.2. Interfacial Tension Between the Liquids..... 13
2.5.3. The Effect of Ions and pH on Zeta Potential of Interfaces..... 13
2.5.4. Rock Surface Properties..... 14
3. STATEMENT OF THE PROBLEM..... 15
4. WETTABILITY MEASUREMENT..... 17

4.1. Procedure..... 17
4.2. Materials..... 17
4.3. Results and Discussion..... 23
5. MEASUREMENT OF INTERFACIAL TENSION..... 33
5.1. Materials..... 33
5.2. Procedure..... 33
5.3. Results and Discussion..... 34
6. OIL RECOVERY IN AMOTT CELLS..... 37
6.1. Materials..... 37
6.2. Experimental Setup..... 40
6.3. Core Preparation..... 44
6.4. Results and Discussion..... 44
6.4.1. Core Sample 9/67..... 44
6.4.2. Core Sample 6..... 46
6.4.3. Core Sample K16 (H1)..... 47
6.4.4. Core Sample K1 (H1)..... 48
6.4.5. Core Sample A7..... 49
6.4.6. Core Sample A8..... 50
6.4.7. Core Sample BS..... 51
7. FLOW VISUALIZATION WITH VIDEO CAMERA..... 57
7.1. Materials..... 57
7.2. Experimental Setup..... 57
7.3. Procedure, Results and Discussion..... 61
8. APPLICATION OF X-RAY COMPUTERIZED TOMOGRAPHY..... 81
8.1. Materials..... 81
8.2. Core Preparation..... 82
8.3. Procedure..... 83

8.4. Results and Discussion..... 85
9. CONCLUSIONS..... 93
REFERENCES..... 95
CURRICULUM VITAE..... 103

LIST OF TABLES

TABLES

Table 4.1- Results of XRD analysis for the sandstone sample [55]..... 18

Table 4.2- Composition of the brines..... 19

Table 4.3- Locations of Oil Samples Used. 19

Table 4.4- Properties of the Batı Raman Heavy Oil and Çamurlu Heavy Oil [55]. .. 21

Table 4.5- Composition of the Batı Raman Heavy Oil and Çamurlu Heavy Oil (% by weight) [55]..... 22

Table 4.6- Composition (% by weight) of the oil samples H and K..... 22

Table 4.7- Properties of the oil samples..... 22

Table 5.1- Values of interfacial tension between oil sample H and formation water (FW) and low saline water (LW). 35

Table 5.2- Acid and Base Numbers of the oil samples L and H..... 36

Table 6.1- Physical Properties of the Core Samples..... 38

Table 8.1- Parameters associated to measurements conducted using X-ray tomography. 84

Table 8.2- Multiplications of porosity and oil saturation for the cases in which the sample was saturated with high saline brine and toluene in the first and second part of the experiment (HBTS1, HBTS2) and before and after high saline brine injection (BHB, AHB). 89

LIST OF FIGURES

FIGURES

Figure 4.1- Aphaltene precipitation on 6 μm filtration papers for different toluene and n-decane fractions. Mass percentages of saturates, aromatics, asphaltene and polar (resin) in the mixtures filtrated through the papers: (a) 4.7, 80, 9.8, 4.8 (b) 30, 55.4, 9.8, 4.8 (c) 40, 45.4, 9.8, 4.8 (d) 50, 35.4, 9.8, 4.8 (e) 64.7, 20.7, 9.8, 4.8 21

Figure 4.2- Percentages of water-wet limestone grains for different oil samples and the brine sample the salinity of which is 106.5 g/L. 25

Figure 4.3- Percentages of water-wet limestone grains for different brine samples and oil sample B. 26

Figure 4.4- Percentages of water-wet limestone grains for different brine samples and oil sample D. 26

Figure 4.5- Percentages of water-wet limestone grains for different brine samples and oil sample F. 27

Figure 4.6- Percentages of water-wet limestone grains for different brine samples and oil sample H. 27

Figure 4.7- Percentages of water-wet limestone grains for different brine samples and oil sample J. 28

Figure 4.8- Percentages of water-wet limestone grains for different brine samples and oil sample I. 28

Figure 4.9- Percentages of water-wet limestone grains for different brine samples and oil sample A. 29

Figure 4.10- Percentages of water-wet limestone grains for different brine samples and oil sample C. 29

Figure 4.11- Percentages of water-wet limestone grains for different brine samples and oil sample E. 30

Figure 4.12- Percentages of water-wet limestone grains for different brine samples and oil sample G. 30

Figure 4.13- Percentages of water-wet sandstone grains for different brine samples and oil sample D. 31

Figure 4.14- Percentages of water-wet sandstone grains for different brine samples and oil sample B. 31

Figure 4.15- Percentages of water-wet sandstone grains for different brine samples and oil sample E. 32

Figure 5.1 - Interfacial tensions between oil sample L and brine samples at 70 °C and different pressures. Interfacial tension meter was used to measure the interfacial tensions. 35

Figure 6.1- Plot of flowrate divided by area vs pressure difference divided by length for the core sample labeled as K16 (H1). 38

Figure 6.2- Plot of flowrate divided by area vs pressure difference divided by length for the core sample labeled as K1 (H1). 39

Figure 6.3- Plot of flowrate divided by area vs pressure difference divided by length for the Berea sandstone. 39

Figure 6.4- Magnetic Mixer and Vacuum Apparatus. 41

Figure 6.5- Core Flooding Apparatus. 42

Figure 6.6-The Amott Cell used in the study. 43

Figure 6.7- Imbibition into the core sample numbered as 9/67. 52

Figure 6.8- Imbibition into the core sample numbered as 6. 53

Figure 6.9- Imbibition into the core sample labeled as K16 (H1). 53

Figure 6.10- Imbibition into the core sample labeled as K1 (H1). 54

Figure 6.11- Imbibition into the core sample labeled as A7. 54

Figure 6.12- Imbibition into the core sample labeled as A8. 55

Figure 6.13- Imbibition into the core sample labeled as BS. 55

Figure 6.14- Oil particles suspended beneath the oil/brine interface. 56

Figure 7.1- Top view of the slice 1. 58

Figure 7.2- The mold into which the rock slice was inserted. 59

Figure 7.3- The milling machine used for creating the voids. 59

Figure 7.4- The band emery machine used for smoothing the surface of the rock slice 60

Figure 7.5- Top view of the slice 2. 60

Figure 7.6- Water flooding in an oil-wet rock. Water bubble enlarges inside the oil phase. 62

Figure 7.7- Enlargement of the water bubble inside the oil phase. 62

Figure 7.8- Rupturing of the oil phase during water flooding in a water-wet rock. 62

Figure 7.9- Choke off process. Oil displaces water. 63

Figure 7.10- Jump process. Oil displaces water. 63

Figure 7.11- Top view after 2.50 minutes of injection of toluene at a rate of 6.7 ml/hour. 67

Figure 7.12- Top view after 4 minutes of injection of toluene at a rate of 6.7 ml/hour. 67

Figure 7.13- Top view after 5 minutes of injection of toluene at a rate of 6.7 ml/hour. 68

Figure 7.14- Top view after 6 minutes of injection of toluene at a rate of 6.7 ml/hour. 68

Figure 7.15- Top view after 30 minutes of injection of toluene at a rate of 6.7 ml/hour. 69

Figure 7.16- Top view after 60 minutes of injection of toluene at a rate of 6.7 ml/hour. 69

Figure 7.17- Top view after 20 minutes of injection of toluene at a rate of 0.33 ml/min. 70

Figure 7.18- Top view after 6 minutes of injection of toluene at a rate of 0.99 ml/min. 70

Figure 7.19- Top view after 2.5 minutes of injection of toluene at a rate of 3.1 ml/min. 71

Figure 7.20- Top view after 1 minute of injection of toluene at a rate of 6.7 ml/min. 71

Figure 7.21- Top view after 1 minute of injection of toluene at a rate of 8.8 ml/min. 72

Figure 7.22- Rupturing of the toluene at the narrow section. 72

Figure 7.23- Top view after 10 days of aging in toluene. 73

Figure 7.24- Top view after 60 minutes of injection of the brine sample at a rate of 0.05 ml/min. 73

Figure 7.25- Top view after 120 minutes of injection of the brine sample at a rate of 0.05 ml/min. 74

Figure 7.26- Top view after 4.5 hours of injection of the brine sample at a rate of 0.05 ml/min. 74

Figure 7.27- Top view before injection of distilled water. 75

Figure 7.28- Top view after 30 minutes of injection of distilled water at a rate of 0.05 ml/min. 75

Figure 7.29- Top view after 60 minutes of injection of distilled water at a rate of 0.05 ml/min. 76

Figure 7.30- Top view after 90 minutes of injection of distilled water at a rate of 0.05 ml/min. 76

Figure 7.31- Top view after 3 hours of injection of distilled water at a rate of 0.05 ml/min. 77

Figure 7.32- Top view after 5 hours of injection of distilled water at a rate of 0.05 ml/min. 77

Figure 7.33- Top view before injection of liquid detergent solution. 78

Figure 7.34- Top view after 30 minutes of injection of liquid detergent solution at a rate of 0.05 ml/min. 78

Figure 7.35- Top view after 60 minutes of injection of liquid detergent solution at a rate of 0.05 ml/min. 79

Figure 7.36- Top view after 90 minutes of injection of liquid detergent solution at a rate of 0.05 ml/min. 79

Figure 7.37- Top view after 3 hours of injection of liquid detergent solution at a rate of 0.05 ml/min. 80

Figure 8.1- View of the core sample used in the tomography application. 82

Figure 8.2- Illustration of the spot size, slice thickness and sections on the top view of the core sample. 85

Figure 8.3- CT values at differet sections for the cases in which the sample was saturated with high saline brine and toluene in the first and second experiments (HBTS1, HBTS2) and the sample was fully saturated with high saline brine (HBS). 88

Figure 8.4- CT values at different sections for the cases in which the sample was fully saturated with high saline brine (HBS), after the sample was saturated with toluene (ATS) and before high saline brine injection (BHB). 89

Figure 8.5- Recovery factor with respect to injected pore volume. 90

Figure 8.6- CT readings for the dry core (a), water saturated core (b), water and toluene saturated core (S_w = % 53) (c), before high saline brine injection (d), after high saline brine injection (e) and after sulfated brine injection (f) at L = 1.0 cm. .. 91

Figure 8.7- CT readings for the dry core (a), water saturated core (b), water and toluene saturated core (S_w = % 53) (c), before high saline brine injection (d), after high saline brine injection (e) and after sulfated brine injection (f) at L = 2.0 cm. .. 92

CHAPTER 1

INTRODUCTION

Recovery of oil from reservoirs is achieved following three stages: Primary recovery in which oil is produced by natural energy of the reservoir , secondary recovery which includes injection of brine or gas to maintain the pressure of the reservoir and tertiary recovery also known as enhanced oil recovery (EOR) includes injection of CO_2 or chemicals such as surfactants, polymers. Among these methods, waterflooding has been observed to be most successful because water is abundant in nature, it is easy to inject, it is especially effective in displacing light to medium gravity oils and the process is more economical compared to EOR applications [1].

Initially, water was seen as a tool for pressure support when natural energy of the reservoir was not sufficient to produce desired amount of oil. Later on, it was realized that composition of the injected brine was important as well [1]. Oil recovery in Ekofisk field in Norway was previously estimated as around 18 % of OOIP during the period including formation brine injection and it has been getting close to 50-55 % of OOIP with seawater injection [2]. Low saline brine was injected to Sandstones beginning from early 1990s after realizing that utilization of low saline brine led to more oil production in comparison to production occurred injecting formation brine sample [3].

Carbonate reservoirs constitute around % 50 of proven oil reserves in the world. Carbonate rocks are brittle and can be highly fractured. It was documented in the literature that around 80-90% of the carbonate reservoirs in the world are prefentially

oil-wet. In addition to this, matrix permeability of carbonates is often low and alters between 1 and 10 mD. Thus, oil recovery from carbonate reservoirs is mostly challenging with low oil recovery factors being less than 30%. On the other hand, EOR potential for carbonate reservoirs is high [4].

EOR applications for carbonates are mostly concerned with fractured reservoirs. In such reservoirs, injected brine flows mainly through fractures bypassing the matrix blocks. Spontenous imbibition into matrix blocks is not possible due to low water-wetness of the rock. The effectiveness of waterflooding process depends on the amount of imbibition from fractures to matrix, which is linked to change in capillary forces, wettability. Expensive chemical agents such as cationic surfactants can be used for this purpose. Because the process is not economical, cheaper alternatives have being investigated [5].

One of the ways to increase spontaneous imbibition from fractures into matrix can be utilization of smart water. The method involves tuning ionic composition and salinity of the injected brine for the purpose of improving oil recovery establishing new chemical condition in the reservoir different from that occurred in the existence of formation brine. This study focuses on this subject.

Chemicals existing in natural brines can alter wettability in favorable way. The aim is to determine such chemicals leading wettability change and proper compositions of them in the brine samples. For this purpose, wettability measurements were conducted using Modified Flotation Test (MFT) procedure and the effects of the brine samples chemical compositions of which were determined considering the characteristics of brine samples proved to be beneficial in increasing the water wettability in previous studies on wettability were examined using different oil samples, limestone and sandstone samples. The results of wettability measurements are presented in CHAPTER 4.

Chemicals existing in smart water can have the function of removing adsorbed oil components from the rock surfaces. These brines have lower salinities in comparison

to salinities of formation brines. Possible changes in interfacial tension between the liquids as a result of decrease in salinities should also be clarified. For this purpose, interfacial tension measurements were conducted using two different oil samples and the brine samples having different salinities. In CHAPTER 5, these findings are reviewed with the previous findings to draw a proper conclusion.

Different brine samples were tested for recovery of oil in Amott Cells. Conditions that lead to improvement in recovery in Amott Cells were tried to be determined. The brine sample to be tested in Amott cells was selected considering the results obtained from wettability measurements. The effect of reducing the salinity and using surfactant on spontaneous imbibition was also investigated. The results of Amott tests are presented in CHAPTER 6.

Flow of oil and water in porous media was visualized with video camera. In the first part, prepared limestone samples were tested for their appropriateness for the study and flow types were determined. In the second part, effect of decreasing salinity and utilization of surfactant were determined with the captured views. The subject is discussed in CHAPTER 7.

Core flood tests were conducted to compare effectiveness of injecting the sulfated brine, utilization of which commonly resulted in highest water-wet fractions in the application of Modified Flotation Test (MFT) procedure with the effect of using high saline brine used to saturate the limestone sample. X-ray computerized tomography was applied to observe the changes occurred after injection of each liquid sample and to ensure that the core sample was saturated with same amounts of liquids before the recovery processes. The results are presented in CHAPTER 8.

CHAPTER 2

LITERATURE REVIEW

2.1 Wettability and Smart Water

In terms of oil production, water-wet rocks in which the water phase tends to occupy small pores and cover the rock surface have some advantageous points. The area under the capillary pressure curve is larger in the region where pressure of the oil phase exceeds the pressure of the water phase and the same area is smaller in the region where the pressure of the water phase exceeds the pressure of the oil phase, which means less energy to displace oil. Since the flow of water is restricted to small pores, water relative permeability remains low during the displacement process. The amount of injected water needed to achieve targeted production will be lower with the existence of high water wettability. That oil relative permeability is high for water-wet rocks brings easiness in replacing oil and thus high production rates. Breakthrough, practical (economical) and ultimate residual oil saturations are close to each other. The disadvantageous point is that the residual oil saturation is higher in comparison to residual saturation for intermediate wet rocks because of formation of trapped oil as the oil is ruptured at narrow pore throats. Depending on the degree of the initial wettability, the aim might be to increase water wetness of the rock. [6] [7] [8].

EOR applications for carbonates are mostly dealt with fractured oil-wet reservoirs. Unswept oil volume in matrix is high for these reservoirs as injected brine follows the highly permeable fractures. The oil remained in the matrix can be recovered with

imbibition of brine into the matrix. The aim of the applications is to find solutions to increase spontaneous imbibition into the matrix by means of increasing water wettability. Increase in imbibition of brine into Stevns Klint chalks was reported with utilization of surface active ions, divalent cations calcium, magnesium and sulfate [9]. Increase in recovery with spontaneous imbibition as a result of decreasing the salinity was also reported for different limestone samples [10]. The potential of oil recovery from fractured limestone reservoirs was indicated.

In view of these facts, the basic aim of utilization of smart water is to increase the water wettability of rock/brine/oil systems and to improve oil recovery as a result.

2.2 Wettability Alteration

The degree of wettability is related to the reactivity of oil and water components towards the rock surface. Polar components mostly found in heavier fractions are thought to be the main wettability altering agents in the oil phase. The way to alter wettability to more water-wet is to remove these adsorbed oil components from the rock surface. Wettability alteration can be achieved by using surfactants, changing the ionic composition of the brine, thermally (increasing the temperature) [11] and utilizing nanoparticles.

Surfactants which have the ability to react with adsorbed oil components and remove them from the rock surface can be used for changing wettability apart from being used for decreasing the interfacial tension. Type of surfactant to be used in wettability alteration depends on the rock type. Anionic surfactants are preferable for sandstones as they carry the same charge with the sandstones [12]. Similarly, cationic surfactants are preferable for carbonates. Anionic surfactants can be effective agents in wettability reversal for carbonates as well [13]. On the other hand, non-ionic surfactants were shown to be ineffective [11].

Increase in water wetness of the rocks with temperature may relate to removal of adsorbed oil components as the solubility of them increase with temperature [14], [15]. The contribution of reduction in interfacial tension with increase in temperature

should be considered as well. Alteration in rock surface elecktrokinetic properties with temperature might be another factor [14]. Although these are suggested mechanisms, the subject has not been clear yet [16].

Nanoparticles the size of which range between 1nm-100nm can be easily transported through narrow pore bodies. They have the function of altering wettability adsorbing onto the rock surface and resulting in a new surface having different property from the previously existing surface [17].

This study focuses on the subject of wettability alteration tuning the ionic composition and brine salinity. The main attempt is to change the wettability of rocks to more water-wet. Besides wettability alteration, other mechanisms can be active leading improvement in oil recovery.

2.3 Smart Water in Carbonates

Injection of seawater was proved to be beneficial in oil recovery from Chalk reservoirs in North Sea [18]. The interactions of divalent cations and sulfate ions found in seawater with chalk surface at high temperature are thought to be the reason of such recoveries. Sulfate ions decrease the magnitude of electrokinetic charge at the chalk surface resulting in increase in calcium concentration close to rock surface. The calcium ions at the surface react with carboxylic material adsorbed onto the rock surface and removes them from the rock surface [19]. Similar effect can be expected for magnesium ions. But magnesium ions form strong ion pairs with sulfate ions and thus its effect may be limited. High temperatures around 110 - 120 °C may be needed for separation of magnesium ions to be effective in wettability change [20].

Temperature is an important factor for reactivity of the ions. Temperatures higher than 90 °C may be needed for reactivity of divalent cations toward the calcite surface [20]. Effect of temperature can be reduced increasing the sulfate concentration found in seawater. The factor that increases the reactivity of the divalent cations toward calcite surface can be reduction of zeta potential of calcite surface with increasing the sulfate concentration.

The degree of wettability change depends on the rock type. Chalks having micropores have larger surface areas in comparison to the surface areas of granular limestones. Thus, their reactivity with surface active ions is higher. Both rock types, chalks and granular limestones consists of calcite minerals. Because the mechanism behind wettability alteration is same for both types, an improvement in wettability can also be expected for granular limestones [20].

Dehydration of magnesium and substitution of calcium ions with magnesium ions at the calcite surface brings the formation of $MgCO_3$ which is more soluble than $CaCO_3$. In this case, rock strength decreases more with dispersion of $MgCO_3$ into water and this will result in more compaction of the rock under the effect of confining pressure. The compaction will bring enhancement in oil recovery [21].

Although it was confirmed that high saline water consisting of mainly sulfate and divalent cations improved oil recovery in carbonates, it was observed in some studies that low saline water utilization results in higher oil recoveries in both spontaneous displacement and coreflooding experiments and lower contact angles compared to results obtained with seawater and formation brine utilization[22] [1]. The factor behind improvement in oil recovery with low saline water utilization could be decrease in interfacial tension. Because the salinity of seawater is much lower than typical formation water, the change in interfacial tension should be also considered in the case of replacement of formation brine with seawater.

Carbonate rocks may contain anhydrite. Calcium and sulfate ions can become active with injection of low saline brine into such rocks and dissolution of anhydrite into low saline brine. The efficiency of the process depends on temperature. Thus, a proper temperature should be defined.

Similar to sulfate ions, the trivalent ions, phosphate and borate can be considered as effective components for reducing the electrokinetic charge on the calcite surface [23].

The problem of precipitation of calcium sulfate should be considered as well increasing the sulfate concentration. Precipitation does not only cause decrease in concentration of surface active ions in brine sample but also can cause blockage of pore throats. In the case of mixation of formation brine and seawater, precipitation of $CaSO_4$ was nil at low temperatures but becomes significant after certain values (60 – 100 °C) [18].

2.4 Smart Water in Sandstones

Low saline brines are used as smart waters for sandstones. For low saline water to be effective in wettability reversal, some conditions should be satisfied: Sandstone should be rich in clay content, oil must include polar components which can be either basic or acidic and the brine sample should include divalent cations [24].

Divalent cations forming bridges between clay surface and acidic oil components are replaced with hydrogen ions in case of replacement of formation brine with low saline water. Hydroxyl ions formed as a result of this process, react with both acidic and basic compounds and remove them from the rock surface. The process results in increase in the pH of the brine [25]. In case of existence of typical formation brine, the process is not effective as the concentration of hydrogen is much lower than the concentration of divalent cations. Salinity of the brine should be decreased to a value below 5000 ppm in order to observe sufficient desorption of divalent cations from the rock surface [24].

Type of clay content may be important as recovery is related to cation exchange capacity of the rock. Potential of wettability change is high for the clay minerals having also high cation exhange capacities. For example, low salinity effects can be observed for montmorillonite clays the cation exchange capacity which varies between 70-120 meq/100 g [26] even if the formation brine does not include divalent cations [27].

There are other mechanisms that play role in oil recovery with low saline water utilization. Clays that expose low saline water swell and migrate. Migration of clay

minerals results in increase in water wettability and causes blockage of pore throats. As pore throats are blocked, the injected fluid will be directed to the non-swept portions of the rock and recover the remaining oil there. The process causes decrease in permeability of the rock. Increase in pressure gradients were commonly reported while injecting low saline brines into sandstones [25].

Increase in pH which can be attributed to replacement of divalent cations with hydrogen ions at the clay surface, was commonly observed for low saline brines injected into sandstones. Low saline water can be thought to act as alkaline with increase in pH. But it is not more than 1 pH unit in most situations. It is doubtful that such small change in pH can cause enough decrease in interfacial tension to observe sufficient improvement in oil recovery [25].

2.5 Factors Affecting the Efficiency of Smart Water

The contribution of utilization of smart water to total oil recovery is dependent on numerous factors such as initial wettability of the system, degree of changes in zeta potential of the interfaces as a result of smart water displacement, initial value of interfacial tension between the liquids and change in it at existing condition and rock surface properties.

2.5.1 Initial Wettability

According to the proposed theory, water exists in porous media before accumulation of oil and thus the rock is completely water-wet at this condition. Later on, brine in porous media is replaced with migrating oil. The interactions of oil components with rock surface bring the alteration in the wettability of the rock/brine/oil system. Mechanisms behind wettability alteration and effects of oil properties on wettability should be well-understood for proper estimation of the initial wettability.

2.5.1.1 Wettability Alteration

When brine is in contact with oil, the degree of developed surface charge depends on the chemicals having potentials to interact with the interface. The interface is

screened with other ions attracted to the interface and moving freely in diffuse layer [28].

The water film on the surface of the rock can prevent the oil components adsorbing to the rock surface. For adsorption to occur, oil pressure must exceed disjoining pressure, known as a minimum pressure needed to collapse the water film. It is easier to combine surfaces under the influence of double layers, if they have opposite charges [29].

2.5.1.2 Mechanisms Behind Wettability Alteration

Several mechanisms were proposed to explain wettability alteration for surfaces initially water-wet [30] [31].

Polar oil components can be soluble in brine and their solubility in oil can be low. In this case, these components can penetrate into brine and react with the rock surface. Adsorption amount depends on brine saturation. High brine saturations can completely inhibit the adsorption.

Polar components in the oil can behave as acids or bases by giving or taking protons. Being an acidic or basic compound, they can react with charged rock particles. Silica surfaces negatively charged above pH 2, have preference to react with basic compounds while calcite surfaces positively charged below pH of about 9.5, have preference to react with acidic compounds at reservoir conditions. Apart from acid and base interactions, polar interactions can also be a factor for wettability alteration. The mechanism is highly active when water film does not exist.

The rock surface and liquid interface can be combined even if they have same charges. The example of this case can be seen for oil/brine/sandstone systems. Divalent cations can combine negatively charged rock surface and negatively charged liquid interface by forming bridge between them.

2.5.1.3 Effect of Oil Properties on Wettability Alteration

The degree of wettability alteration depends on the polarity of the oil components and their solubility in the oil phase. These polar components are largely found in heavier fractions of oil, such as asphaltenes and resins. A positive correlation can be seen between asphaltene and resin content and wettability alteration. There is not a direct correlation between adsorption amount and wettability alteration as the alteration depends also on acid and base contents of the oil [32]. Rapid increase in oil wettability can be observed at the point of asphaltene precipitation [33].

Solubility of asphaltenes in crude oil remains constant over a wide range of temperature but decreases as the temperature approaches to the bubble point. In the zone above the bubble point, evaporation of saturates causes increase in asphaltene solubility as the temperature increases or pressure decreases [34] [35].

Polar activity of asphaltenes is high at the interface when their solubility depending on the saturates concentration in oil is low [36]. Accumulation of asphaltene does not only alter the wettability but also changes interfacial tension. Reduction in interfacial tensions with asphaltene accumulation on the brine/oil interface was noted [37].

Adsorption of asphaltene onto the rock surface can be prohibited increasing the salinity of the brine thus forming a strong film [38].

For carbonates, oil wettability increases as acid number of oil increases [39]. Similarly, oil wettability increases as base number of oil increases for silica surfaces. In other words, low water wettability can be expected in the case of high acid number to base number ratio for carbonates and in the case of low acid number to base number ratio for silica [36].

Based on the experimental works, it seems that temperature has minor effect on wettability and wettability is mainly determined with chemical properties of oil, brine and rock surface [40] [39].

2.5.2 Interfacial Tension between the Liquids

The value of interfacial tension between oil and brine is dependent on the salinity of the brine, temperature and pressure.

Decrease in interfacial tension between alkanes and different brine samples (including single component) with decrease in salinity of the brine samples was commonly reported in the literature [41] [42] [43] [44]. The situation was different for crude oils. There are reports indicating decrease in interfacial tension with decrease in salinity [45]. Contrary to these observations, increase in interfacial tension with decrease in salinity was also noted for some crude oils [46]. In the study of Vijapurapu and Rao [47], existence of a critical limit for salinity to obtain low interfacial tension was reported. It seems that the effect of salinity on interfacial tension between crude oils and brines is dependent on oil properties.

Decrease in interfacial tension with decreasing pressure and increasing temperature was commonly reported in the literature [48] [49]. The subject is still unclear as the effect of temperature can be different depending on the value of pressure [50], oil type (whether mineral oil or crude oil) and brine salinity [26].

2.5.3 The Effects of Ions and pH on zeta potential of Interfaces

The value of the zeta potential of interfaces depends on the ionic composition of the liquids and pH of the solution. For example, increasing the Ca^{2+} and Mg^{2+} concentration in the brine sample or exchanging the NaCl with $CaCI_2$ or $MgCI_2$ increases zeta potential of oil/brine interface making it a positive value. Similarly, increasing SO_4^{2-} concentration in the brine sample or exchanging the NaCl with Na_2SO_4 decreases zeta potential of oil/brine interface making it negative [51] [5] [52]. The effect of pH on zeta potential is different. As pH increases, magnitude of zeta potential decreases upto a point of minimum and increases after that point [53].

2.5.4 Rock Surface Properties

Although surface active ions have potential to increase water wettability, the effect depends on the properties of the rock samples. Decrease in contact angles on smooth surfaces as a result of using these surface active ions may not be representative for reservoir rocks. Branches, side pore mouths and void spaces can affect the interface shape. A wide range of contact angles can be possible at sharp edges, thus there is the possibility that contact lines mainly locate at sharp edges. Another reason for the alteration of contact angle is the surface roughness which decreases the apparent contact angles less than 90° while increasing them when they are greater than 90° [7].

CHAPTER 3

STATEMENT OF THE PROBLEM

Primary production leaves abundant of oil unrecovered. This case is more severe in fractured, neutral-wet to oil-wet reservoirs. There is a need for enhanced oil recovery for such reservoirs. One of these EOR techniques could be change in wettability of carbonate reservoir from oil-wet to water-wet. It can be achieved by injection water capable of removing oil components from the rock surface with surface active ions, which is actually the main idea behind smart water utilization. By using smart water, it is aimed to alter liquid/rock and liquid/liquid interactions by tuning composition and salinity of the injected brine in a way that improvement in oil recovery can be achieved.

The aim of this study is to test the effect of brine samples having different composition and salinities on oil recovery, wettability and interfacial properties in a laboratory environment. Brine samples will be prepared considering the characteristics of the samples proved to be effective in oil recovery. It is planned to clarify the mechanism behind improved oil recoveries which are achieved with smart water utilization.

.

CHAPTER 4

WETTABILITY MEASUREMENT

4.1 Procedure

Modified Flotation Test (MFT) procedure was utilized for comparison of the wettability [54]. According to the procedure, grounded rock sample was first sieved to 53 microns. 0.2 g of the sieved sample and 10 ml water were added to a test tube. The rock particles were aged in the brine for two days. Then, brine sample was separated, was saved in another tube and 3 ml of the oil sample was added to the test tube including rock particles. The rock sample was aged in the oil phase for two days. During this period, the mixture was stirred two times in a day. Then, saved brine was added back to the mixture, stirred vigorously and kept to settle for one day. Finally, oil and brine samples and rock particles locating in the oil phase were separated from the test tube and remaining rock particles located at the bottom of the test tube and considered to comprise water-wet fractions were dried and weighted. The ratio of the weight of these particles to total weight (0.2 g) was taken as the water-wet fraction of the sample.

4.2 Materials

The limestone sample includes small amounts of quartz and feldspar apart from the calcite mineral. Petrography analysis did not indicate any water soluble components in the sample.

The other rock sample was Berea sandstone having low clay content (Table 4.1).

Different salinities were tested in wettability measurements (Table 4.2). The brine samples termed as FW indicate formation brines. The brine named as SW indicates seawater. Mass of dissolved solids in the brine termed as SW*4SO_4 is same with mass of dissolved solids in SW but sulfate concentration in SW*4SO_4 is four times of sulfate concentration in SW. It was prepared by adding Na_2SO_4 and removing NaCl from the salt mixture existing in SW. Effectiveness of sulfate in wettability preference was tested by comparing SW with SW*4SO_4. $MgSO_4$ and Na_2SO_4 solutions and SW*4SO_4 have same sulfate concentrations. By doing so, activity of cations were compared in the case of existence of high sulfate concentrations. The brine termed as SW0NaCl represents seawater from which NaCl is removed and the brine termed as DW is distilled water. TDS refers to total dissolved salts in the brine samples.

Oil samples were brought from different locations in southeastern Turkey and Middle East (Table 4.3).

Table 4.1- Results of XRD analysis for the sandstone sample [55].

	Wt %	**Mineral**
Clay	3	Smectite
		Chlorite
		Illite
		Kaolinite
Non-Clay	97	Quartz
		Calcite
		Plagioclase
		K-feldspar

Table 4.2- Composition of the brines.

Ions	FW_1 (mol/L)	FW_2 (mol/L)	FW_3 (mol/L)	FW_4 (mol/L)	$SW*4SO_4$ (mol/L)	SW (mol/L)	SW0NaCl (mol/L)
Cl^-	3.766	3.218	1.883	1.318	0.298	0.472	0.118
HCO_3^-	0.006	0.000	0.003	0.002	0.000	0.000	0.000
SO_4^{2-}	0.001	0.002	0.001	0.001	0.095	0.024	0.024
Mg^{2+}	0.171	0.137	0.086	0.060	0.046	0.046	0.046
Ca^{2+}	0.666	0.360	0.333	0.233	0.014	0.014	0.014
Na^+	2.100	2.228	1.050	0.735	0.370	0.401	0.048
TDS (g/L)	213.0	180.0	106.5	74.5	29.9	29.9	9.2

Table 4.3- Locations of Oil Samples Used.

Oil Sample	Location
A	Kirkuk
B	Kuwait
C	Turkey (Beykan Field)
D	Iranian
E	Turkey
F	Turkey
G	-
H (Mixture)	Turkey (Batı Raman Field)
I	n-decane
J	Toluene
K (Mixture)	Turkey (Çamurlu Field)
L	Turkey (Bozhüyük)

For oil samples H and K, Batı Raman and Çamurlu heavy oils the property and the compositions of which were given in Table 4.4 and Table 4.5 were selected to be main wettability alterating agents. The ratio of base number to acid number in these oils is high and they have very high viscosity. In order to reduce the viscosity of the samples, toluene and n-decane were added. Toulene being an aromatic compound increase the solubility of asphaltenes found in the heavy oils while n-decane, a nonpolar compound reduces it. Considering that fact, toluene and n-decane concentrations in the solution were determined taking the limit at which the precipitation of asphaltenes on 6 μm filtration paper was avoided.

Asphaltene precipitations on filtration papers for different solutions are indicated with ovals in Figure 4.1 for oil sample H. The solutions were prepared altering n-decane and toluene fractions while keeping the asphaltene and resin fractions constant. The pictures in part (a) and in part (d) were taken after filtrating the solution which did not include n-decane and after filtrating the solution which did not include toluene, respectively. As it can be seen from the figure, asphaltene precipitation increases as n-decane concentration increases. The precipitation was not observed in part (a) and (b).

Compositions of the oil samples H and K were shown in Table 4.6.

Densities, acid and base numbers which are influencing factors for wettability and can be used as indicatives for the differentiation in wettability as different oil samples are tested are shown in Table 4.7. The method used for the measurement of densities is designated as ASTM D 4052 and is known as oscillating u- tube method and the methods used for the measurement of acid and base numbers are designated as ASTM D 664-11a, ASTM D2896-11 and include potentiometric titration and potentiometric perchloric acid titration, respectively. The devices used for the measurement of densities, acid and base numbers are Anton Poor DMA 4500 and Metrohm 848 Titrino plus, respectively.

As can be seen from Table 4.7, most of the oil samples have high base number and low acid number. The oil sample G having high acid number and low base number constitutes an exception. The oil samples D, H and K are light oils. Other oil samples listed in the table are medium oils.

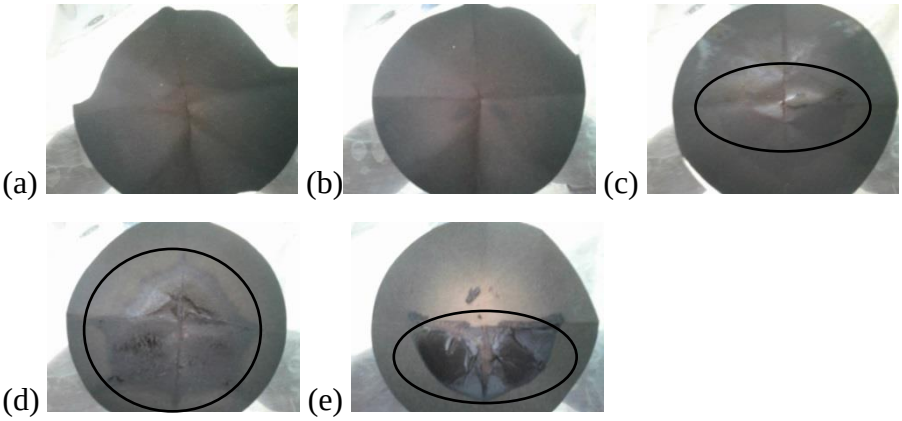

Figure 4.1- Aphaltene precipitation on 6 µm filtration papers for different toluene and n-decane fractions. Mass percentages of saturates, aromatics, asphaltene and polar (resin) in the mixtures filtrated through the papers: (a) 4.7, 80, 9.8, 4.8 (b) 30, 55.4, 9.8, 4.8 (c) 40, 45.4, 9.8, 4.8 (d) 50, 35.4, 9.8, 4.8 (e) 64.7, 20.7, 9.8, 4.8

Table 4.4- Properties of the Batı Raman Heavy Oil and Çamurlu Heavy Oil [55].

Sample	Viscosity (cP) at (60 °C)	Density (g/cm^3) at 15°C	API Gravity at 15 °C	TAN (mgKOH/g)	TBN (mgKOH/g)
Batı Raman Heavy Oil	800.9	0.98635	12.6	0.33	5.59
Çamurlu Heavy Oil	1134.4	1.00615	9.5	0.81	6.12

Table 4.5- Composition of the Batı Raman Heavy Oil and Çamurlu Heavy Oil (% by weight) [55].

Sample	Saturates	Aromatics	Asphaltene	Polar (Resin)
Batı Raman Heavy Oil	11.75	51.72	24.56	11.97
Çamurlu Heavy Oil	9.89	53.62	26.06	10.44

Table 4.6- Composition (% by weight) of the oil samples H and K.

Sample	Saturates	Aromatics	Asphaltene	Polar (Resin)
H	30	55.4	9.8	4.8
K	48.0	41.1	7.8	3.1

Table 4.7- Properties of the oil samples.

	Density (kg/m^3)	TAN (mgKOH/g)	TBN (mgKOH/g)
B	880.3	<0.01	1.34
C	871.2	<0.01	1.73
D	864.0	<0.01	1.35
F	871.1	<0.01	1.33
G	902.2	1.57	0.22
H	853.6	<0.01	1.91
K	846.0	<0.01	1.82
L	891.8	0.22	2.87

4.3 Results and Discussion

Figure 4.2 shows water-wet fractions of the limestone particles for different oil samples. Water-wet fraction is highest for n-decane which is a non-polar liquid. Rock particles exposing to toluene the polarity of which is higher than n-decane, shows more oil-wet characteristics. Water wettability of rock particles mixed with Iranian light oil is low. This is an expected result because light oils lack heavy fractions whose polarities are high. The low water- wet fraction was obtained with oil sample G which has high acid number (1.57 mg KOH/g) and almost nil base number (0.22 mg KOH/g). This is analogous with the fact that limestone particles show more oil wet characteristics if the acid number to base number ratio is higher. Although asphaltene and resin fraction in oil sample H is high, oil wettability of rock grains mixed with that sample is not high. This can be attributed to high ratio of the base number to the acid number in that oil.

Figures 4.3 – 4.15 show the results of wettability measurements conducted at ambient conditions. Y axis in the figures indicates percentage of rock grains that dispersed in the brine samples, in other words water-wet fractions. Each figure consists of the results of measurements conducted using an oil sample specific for that figure and different brines.

The figures were separated into two groups based on water-wet fractions obtained using formation brine samples. One group including Figures 4.3 – 4.8 shows water-wet fractions higher than 0.5 while the other group including Figures 4.9 - 4.12 shows lower water-wet fractions.

Figures 4.3- 4.8 show the result of wettability measurements for the oil samples B, D, F, H, J, I. The highest water-wet fraction was obtained using the brine sample, SW*4SO_4 being rich in both sulfate and divalent cations. SW and SW0NaCl having lower sulfate concentrations and Na_2SO_4 solution lacking of divalent cations show less water-wet characteristics. Although $MgSO_4$ solution is rich in divalent cations and sulfate, water-wet fraction is low for this brine sample. This can be attributed to

low ionization of $MgSO_4$ in water at ambient conditions. Much higher temperatures are needed for enough ionization to observe the effect. Water-wet fraction for the brines SW*4SO_4, SW, SW0NaCl and Na_2SO_4 solution are shown to be higher compared to water-wet fraction of FWs indicating the effect sulfate ion and cations. Rather than divalent cations, adding sodium to brine also increases water-wet fraction, the effect of which can be seen with comparison of SW and SW0NaCl and with the results obtained using Na_2SO_4 solution. It is commonly observed from the figures that utilizing distilled water reduces water-wet fraction in comparison to water-wet fraction observed in formation brine samples. Another common observation is the lower water-wet fraction occurred when FW_2 was used in comparison to other formation brine samples. The fractions of the ions found in FW_2 were different from the fractions in other formation brine samples. The low fraction of Ca^{2+} in FW_2 is possibly the reason of such observation.

Figures 4.9 – 4.12 show the results of wettability measurements for the oil samples A, C, E, G. The common characteristic represented in the figures is the low water-wet fraction. In the case of using oil sample A, it was figured out that using SW and SW0NaCl was not helpful in increasing the water-wet fraction as distinct from the cases in which fraction of the amount in formation brine samples was higher than 0.5. On the other hand, water-wet fractions were increased utilizing SW*4SO_4 and Na_2SO_4 solution having sulfate concentations 4 times of the sulfate concentrations found in SW and SW0NaCl. The study shows the importance of increasing the sulfate concentration for that oil for obtaining more water-wet system. For oil sample G, water-wet fraction could not be increased even using the brine, SW*4SO_4 rich in both sulfate and divalent cations. The specific characteristic of this oil is that it has high acid number and low base number. It was probable that using surface active ions (sulfate and divalent cations) was not helpful in preventing the acidic substances in the oil phase reacting with calcite. Higher temperatures may be needed to increase the effectiveness of divalent cations. Although water-wet fractions were low for oil sample E, the effects of smart waters are similar to the effects seen for cases in which fractions of the amount in formation brine samples are higher than 0.5.

Figures 4.13 – 4.15 show the results of wettability measurements for the sandstone sample. 1 M NaCl, $MgCl_2$ and $CaCl_2$ solutions were tested with oil samples B, D and E. In all tests, water-wet fractions are highest when NaCl was used as a solute. It is seen that divalent cations, Ca^{2+} and Mg^{2+} increases oil wettability. Distilled water, which is low saline water in this case, was not helpful in increasing the water wettability possibly due to low clay content of the sandstone sample (Table 4.1).

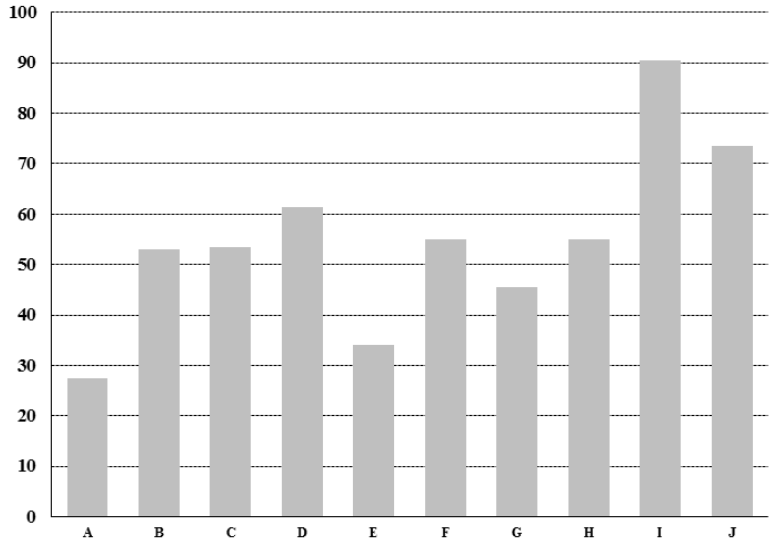

Figure 4.2- Percentages of water-wet limestone grains for different oil samples and the brine sample the salinity of which is 106.5 g/L.

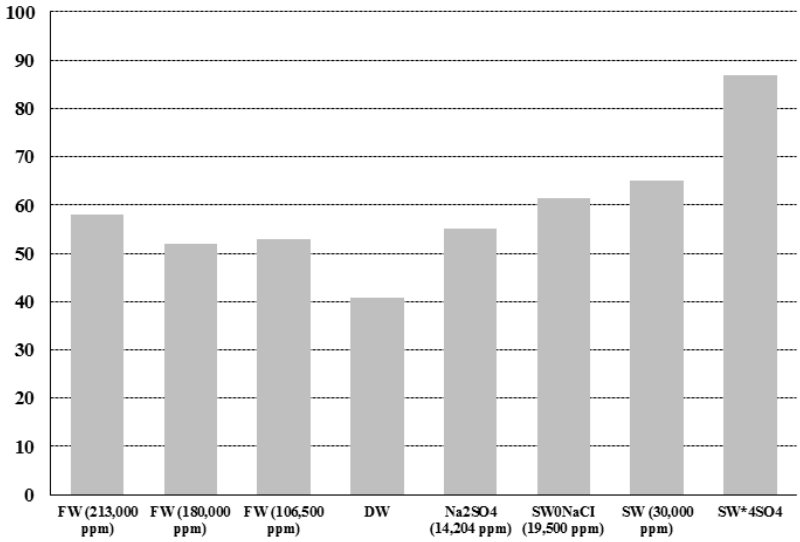

Figure 4.3- Percentages of water-wet limestone grains for different brine samples and oil sample B.

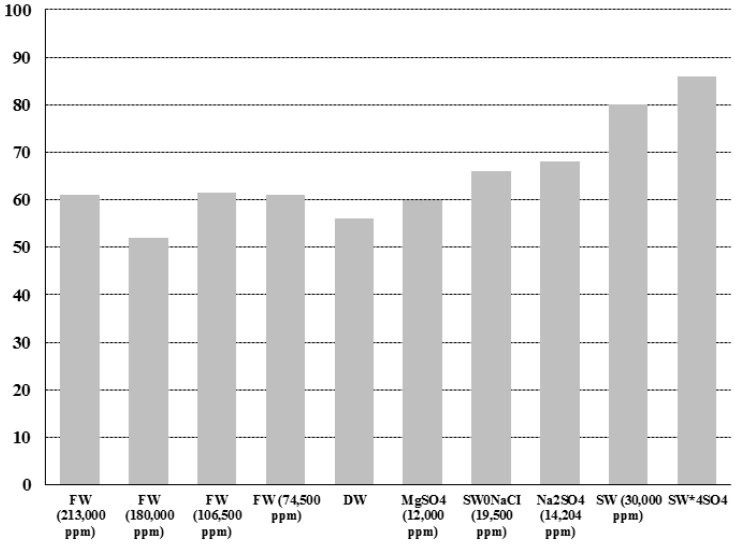

Figure 4.4- Percentages of water-wet limestone grains for different brine samples and oil sample D.

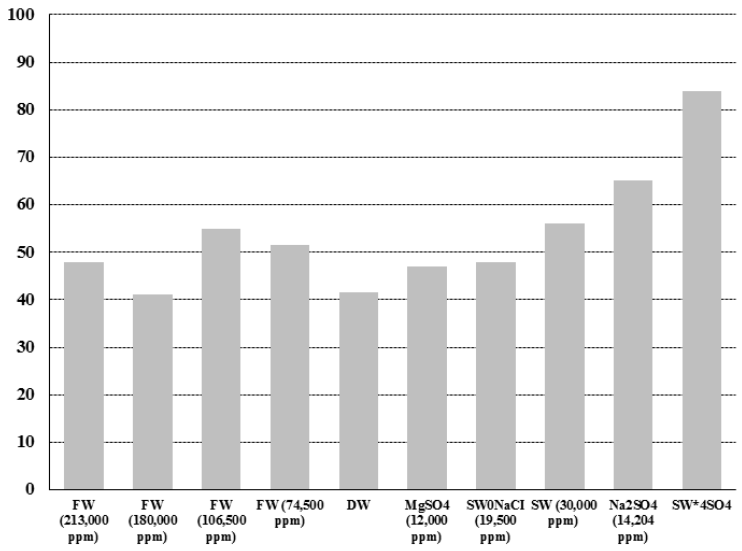

Figure 4.5- Percentages of water-wet limestone grains for different brine samples and oil sample F.

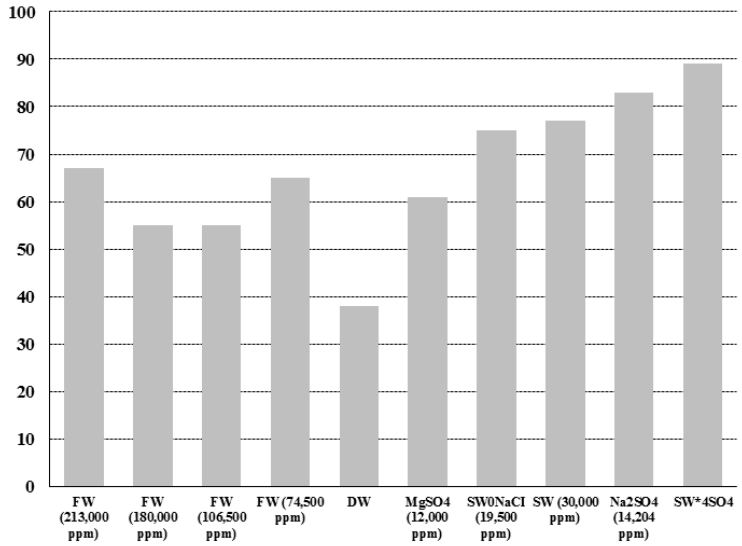

Figure 4.6- Percentages of water-wet limestone grains for different brine samples and oil sample H.

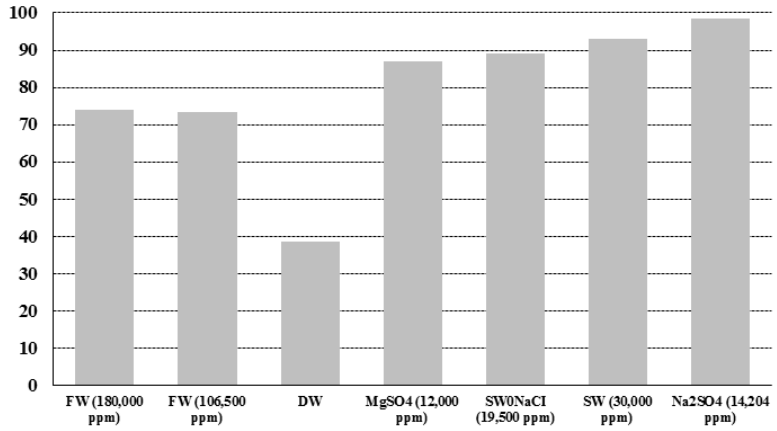

Figure 4.7- Percentages of water-wet limestone grains for different brine samples and oil sample J.

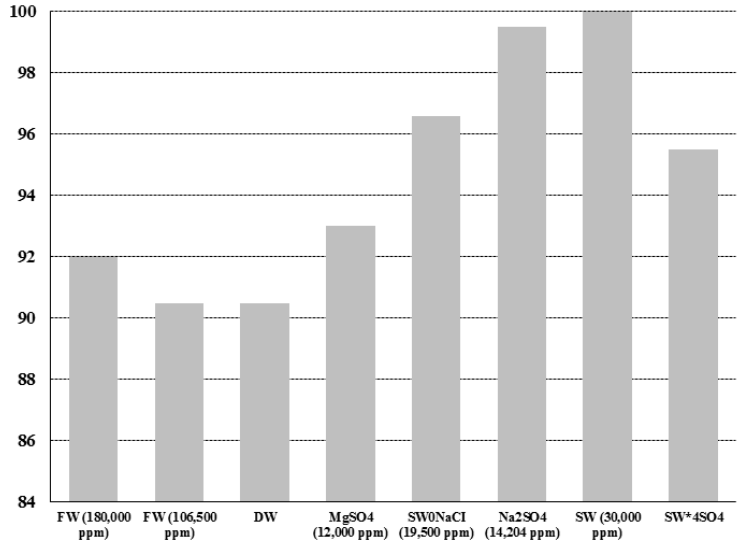

Figure 4.8- Percentages of water-wet limestone grains for different brine samples and oil sample I.

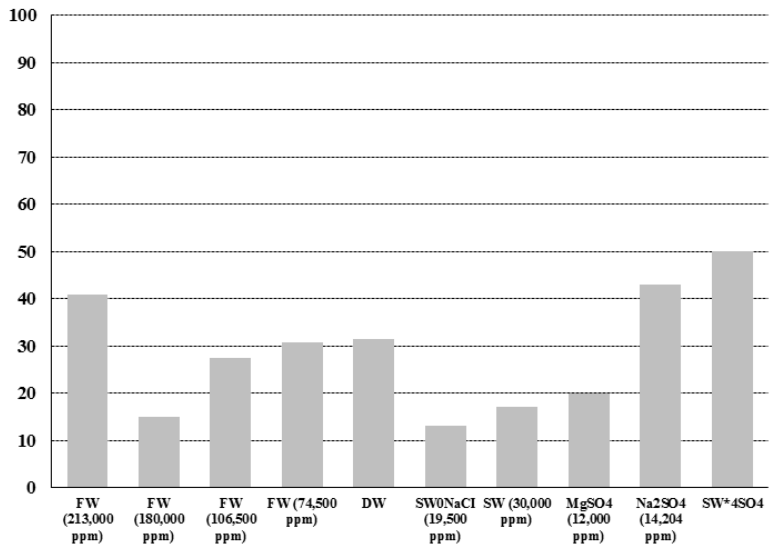

Figure 4.9- Percentages of water-wet limestone grains for different brine samples and oil sample A.

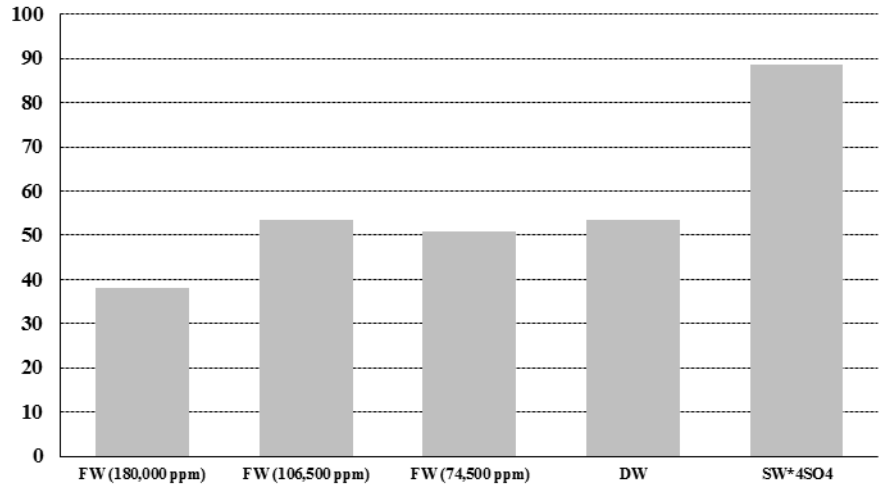

Figure 4.10- Percentages of water-wet limestone grains for different brine samples and oil sample C.

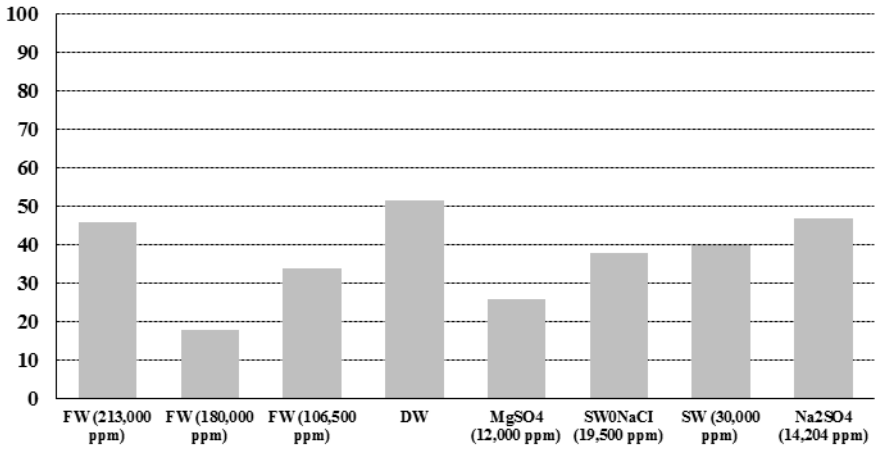

Figure 4.11- Percentages of water-wet limestone grains for different brine samples and oil sample E.

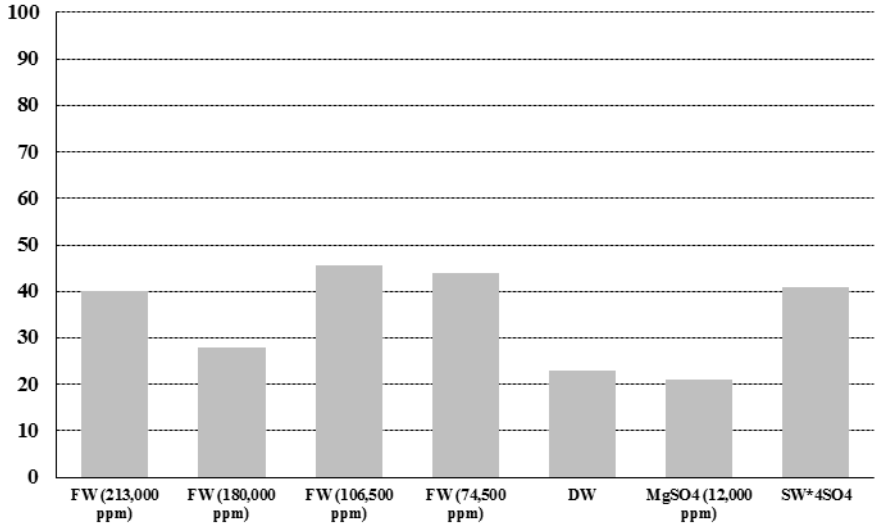

Figure 4.12- Percentages of water-wet limestone grains for different brine samples and oil sample G.

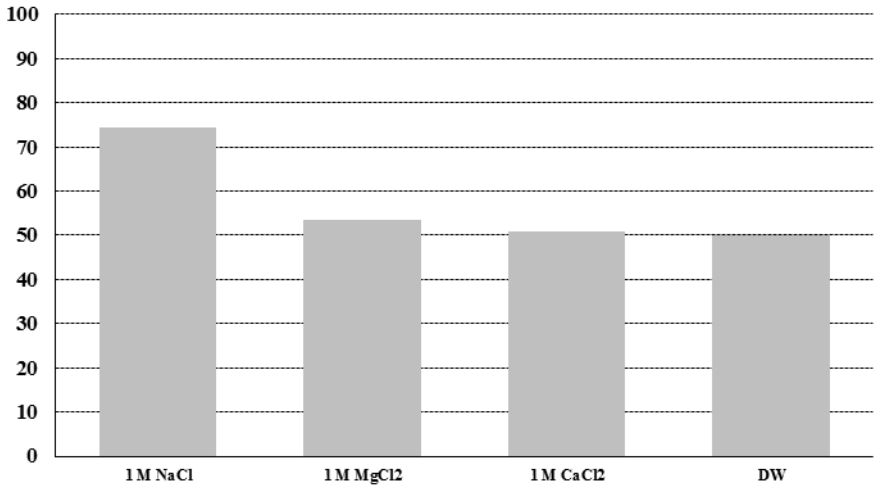

Figure 4.13- Percentages of water-wet sandstone grains for different brine samples and oil sample D.

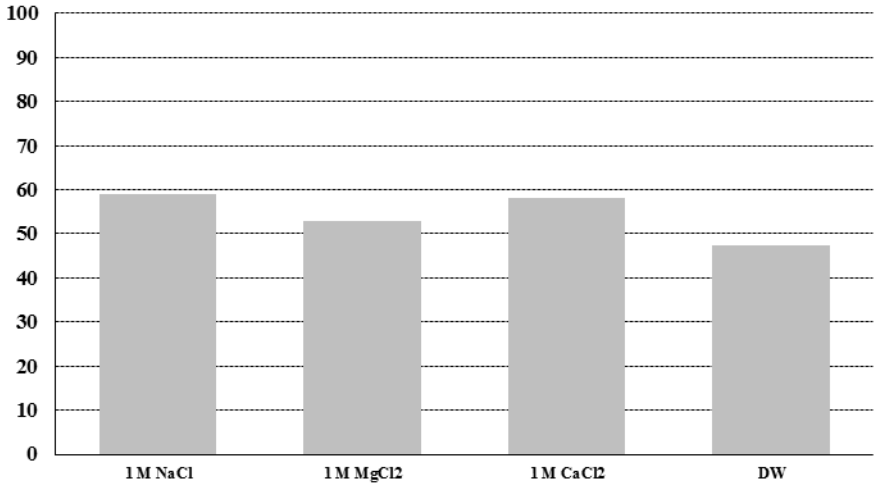

Figure 4.14- Percentages of water-wet sandstone grains for different brine samples and oil sample B.

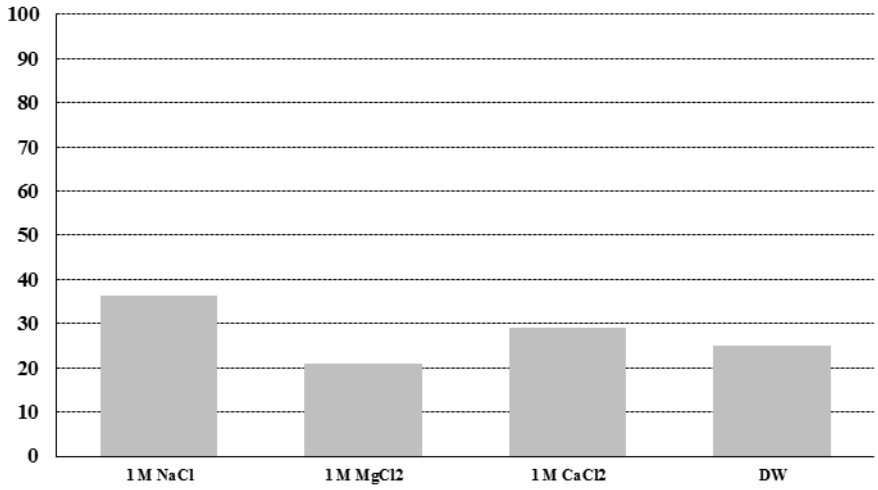

Figure 4.15- Percentages of water-wet sandstone grains for different brine samples and oil sample E.

CHAPTER 5

MEASUREMENT OF INTERFACIAL TENSION

5.1 Materials

Interfacial tensions between oil sample L (Table 4.3) and brine samples FW_3 (TDS=106.5 g/L), SW*4SO_4 (Table 4.2) and distilled water (DW) were measured with interfacial tension meter (IFT 700). Interfacial tension between oil sample H (Table 4.3) and brine samples FW_3 (Table 4.2) and DW was measured with ring tensiometer.

5.2 Procedure

In the interfacial tension measurement conducted with tension meter, oil droplet was formed in a chamber filled with water with a method known as rising drop which includes upward movement of the phase with the help of a needle. After the droplet stabilized, the image was captured to be used in the calculation of interfacial tension. Interfacial tensions were calculated using Laplace – Young equation which correlates the shape of the droplet with interfacial tension and gravitational force.

The ring tensiometer consists of a ring which was immersed into the brine sample and was kept as close as possible to the interface while remaining in the brine sample. Tension was applied by turning the arm of the tensiometer. The tension value at the moment the interface ruptured and the ring released from the interface was recorded as interfacial tension. Before starting the measurement, oil droplets around the needle was removed with a stick.

5.3 Results and Discussion

The result of the interfacial tension measurement conducted with tension meter is shown in Figure 5.1. As it can be seen from the figure, the interfacial tensions between the oil sample and DW and SW*4SO_4 are higher than interfacial tension between the oil sample and FW_3, indicating that decreasing the salinity resulted in increase in the interfacial tension for that oil sample. Tension measured with the brine sample SW*4SO_4 was almost same with the tension value for DW.

Table 5.1 shows the result of interfacial tension measurements conducted with the ring tensiometer. The liquids were kept in the chamber for equilibrium and the measurement was conducted at different times. As it can be seen from the table, lowering the salinity caused increase in the interfacial tension similar to the case observed for the oil sample I.

Despite the common reporting of decrease in interfacial tension with decrease in salinity in the literature, the tension was inversely related to salinity for the oil samples tested in this study. The common property of the oil samples is that they have high base numbers and low acid numbers (Table 5.2). This might bring out the positive electro kinetic charge at the interface which attracts chloride ions that weaken the water structure. As a result of this phenomenon, interfacial tension decrease with increasing the salinity and thus chloride concentration.

Increase in salinity did not cause any noticeable change in interfacial tension for the brine samples, SW*4$S0_4$ and DW. This might be because of replacement of chloride ions with SO_4 ions strengthening water structure at the interface.

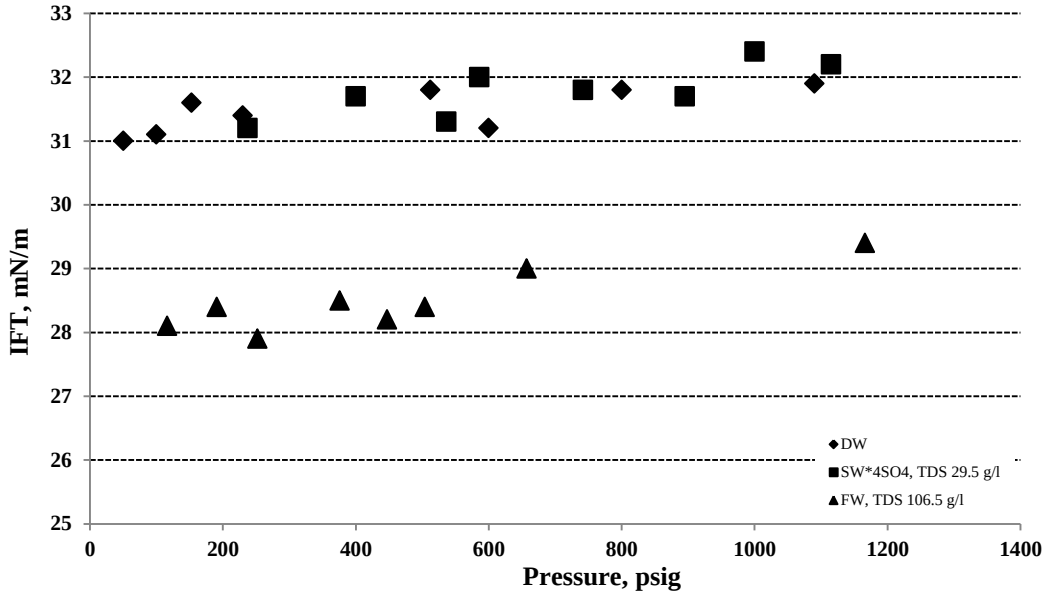

Figure 5.1 - Interfacial tensions between oil sample L and brine samples at 70 °C and different pressures. Interfacial tension meter was used to measure the interfacial tensions.

Table 5.1- Values of interfacial tension between oil sample H and formation water (FW) and low saline water (LW).

Duration (days)	Temperature (°C)	IFT between oil and FW (dynes/cm)	IFT between oil and LW (dynes/cm)
1	15	27.4	37.0
2	19.0	21.6	35.7
3	19.4	20.0	35.0

Table 5.2- Acid and Base Numbers of the oil samples L and H.

Sample	TAN (mgKOH/g)	TBN (mgKOH/g)
L	0.22	2.87
H	<0.01	1.91

CHAPTER 6

OIL RECOVERY IN AMOTT CELLS

6.1 Materials

Physical properties of the core samples used in the study are listed in Table 6.1. The core samples labeled as 9/67, 6, K16 (H1), K1 (H1), A7 and A8 are limestone and the core sample labeled as BS is the Berea sandstone. The porosity values listed in the table were determined calculating the differences between the weights of dry and brine saturated cores and densities of the brines needed for the porosity calculations were estimated dividing to total mass to total volume which was measured after the addition of salts to distilled water with a known volume. Figures 6.1 – 6.3 show the plots of pressure differences divided by lengths vs flowrates divided by areas for determination of permeability of the core samples, K16 (H1), K1 (H1) and BS. The permeability of the core samples 9/67 and 6 were not measured but provided. Permeability of the core samples, A7 and A8 were not able to be measured since increase in inlet pressure was not observed during the flooding process, which indicates that these core samples are highly permeable. Initial oil saturations prior to spontaneous imbibition experiments are also shown in Table 6.1.

Table 6.1- Physical Properties of the Core Samples.

Sample	Length (cm)	Diameter (cm)	V_b (cm^3)	Dry Weight (g)	Porosity (%)	Permeability (mD)	S_{oi} (%)
9/67	6.2	3.78	69.58	142.706	26	161	64
6	5.3	3.6	53.95	114.666	32	123	73
K16 (H1)	6.8	3.78	76.31	154.613	20	452	40
K1 (H1)	5.9	3.78	66.21	149.276	14	48	28
A7	5.85	3.49	56.28	99.681	42	-	40
A8	5.7	3.48	54.22	100.014	41	-	43
BS	6.88	3.78	77.21	168	23	80	59

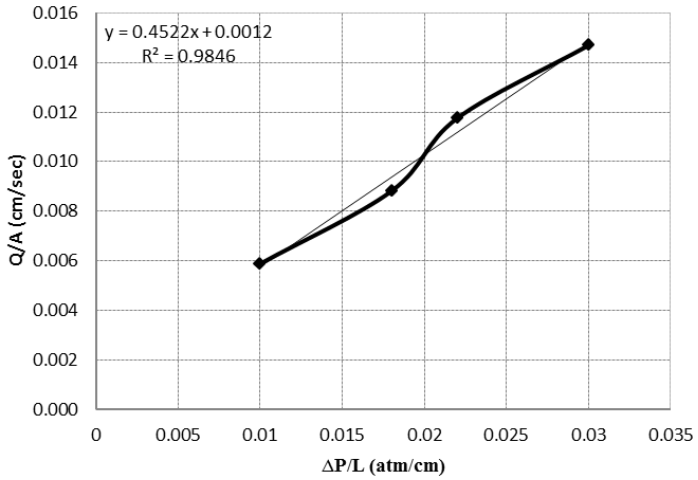

Figure 6.1- Plot of flowrate divided by area vs pressure difference divided by length for the core sample labeled as K16 (H1).

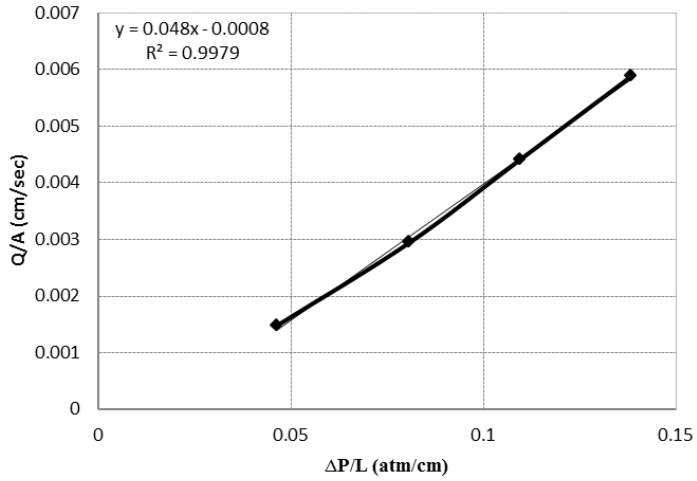

Figure 6.2- Plot of flowrate divided by area vs pressure difference divided by length for the core sample labeled as K1 (H1).

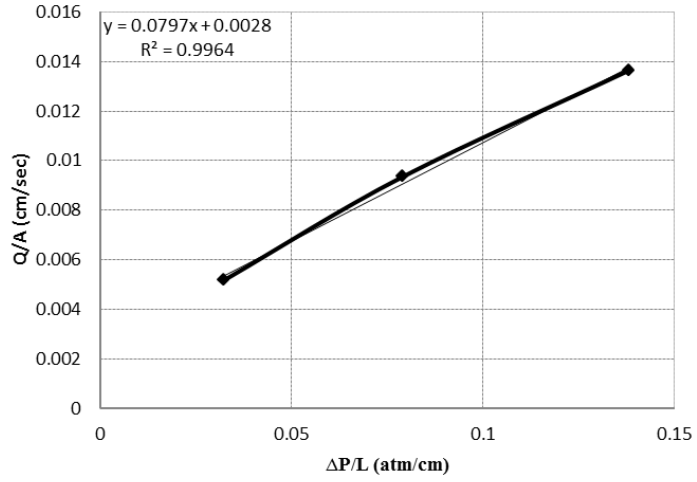

Figure 6.3- Plot of flowrate divided by area vs pressure difference divided by length for the Berea sandstone.

Oil Samples H and K (Table 4.3), n-decane and toluene, the brine samples FW_3 and FW_4 (Table 4.2), 200 g/L NaCl solution and distilled water were used to saturate the core samples. The purpose of using low saline formation brine samples, FW_3 and FW_4 and distilled water was to diminish the effects arising from alteration in interfacial tension between the liquids as a result of change in salinity. By doing so, it was possible to relate the potential of the ions in removing the oil components from rock surface to oil recovery. The purpose of using high saline brine, 200 g/L NaCl solution was only to check the effect of reduction in interfacial tension arised from the change in salinity on oil recovery. Heavy oil was added to n-decane and toluene mixture in the preparation of oil Samples H and K to increase the polarity of the mixture and stearic acid having the function of increasing the oil wetness of the carbonates was added to n-decane. By doing so, oil samples having different polarities could be tested in the experiment.

In the spontaneous imbibition experiments, the brine sample, SW*4SO_4, Na_2SO_4 solution (Table 4.2), distilled water and liquid detergent were tested after imbibition of the brine samples used to saturate the core samples. The brine sample, SW*4SO4 and the Na_2SO_4 solution were selected as highest water wet fractions were obtained using them in the wettability measurements. The purpose of using distilled water and liquid detergent composed of % 5 – 15 anionic surfactant, <% 5 nonionic surfactant and preservatives which are benzisothiazolione, phenoxyethanol and geraniol was to change the interfacial tensions between the liquids and to observe any increment in oil recovery as a result.

6.2 Experimental Setup

The first part of the experimental work included setting up the vacuum and core flooding apparatuses and testing them.

Magnetic mixer was utilized to dissolve the salts in the water. Saturation of the cores with brine solutions and vacuum pumping were performed simultaneously to ensure that gas had fully left the core sample (Figure 6.4). Cleaned and dried core samples

were placed into the filtering flask and were evacuated. Then, water was dropped off from seperatory funnel that is connected to the upper entrance of filtering flask while evacuation was continued. The process continued until brine level exceeds the height of the core. Then, the core samples were left in the brine solution for establishing chemical equilibrium between brine and core sample.

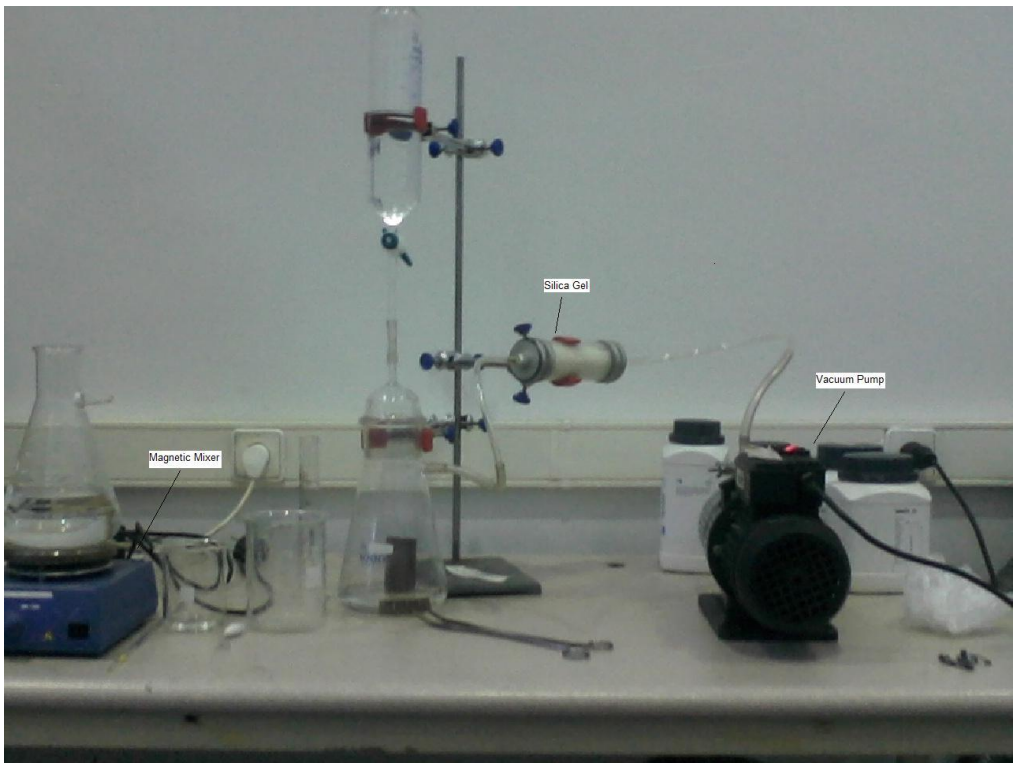

Figure 6.4- Magnetic Mixer and Vacuum Apparatus.

A new core apparatus was set up to perform core flooding tests (Figure 6.5). The apparatus consists of a metering pump, core holder, piston cell, pressure transducers,

thermocouples and valves. The core holder and piston cell were located in an oven to carry out the experiments at the desired temperature. Three pressure transducers were utilized, two of them were used for measuring pressures at the inlet and outlet of the core holder, the other one was used for measuring the confining pressure. The transducers were connected to the computer for continuous recording of the measured data. The core holder includes rubber sleeve which wraps the core as confining pressure exceeds the inlet pressure. This wrapping of the core prevents the injected fluid passing around the core sample. Injection of the fluid with constant pressure and constant rate needed for measuring the permeability of the core, saturating the sample with oil and recovering the oil remained in the core with waterflooding could be established with metering pump. Correctness of the pressure transducers was checked with a calibration device.

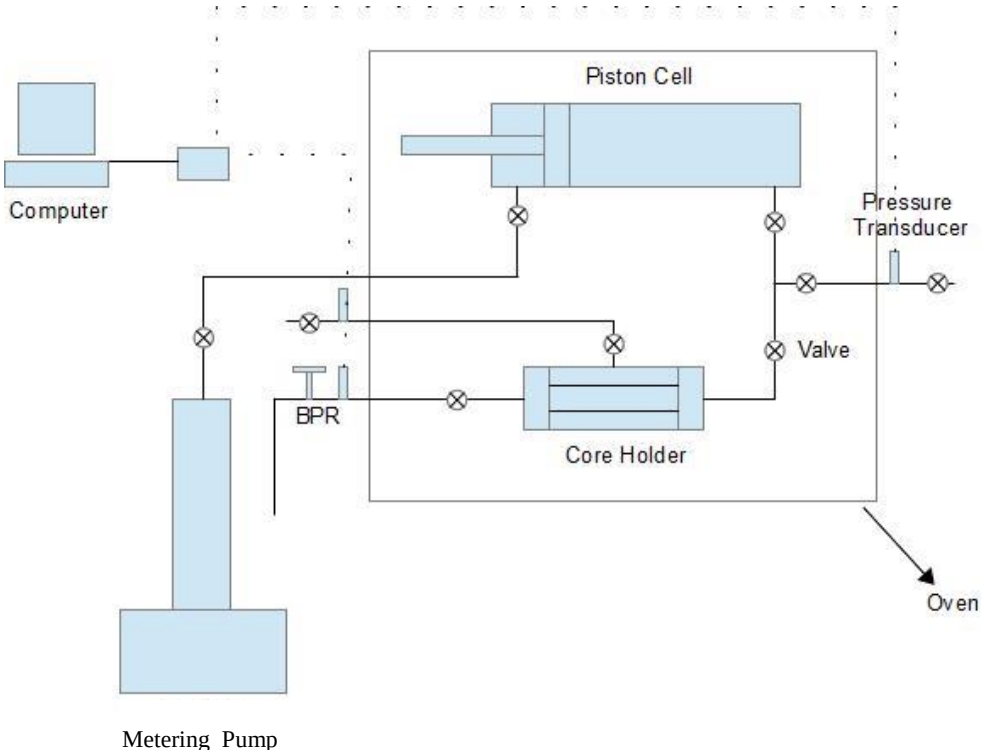

Figure 6.5- Core Flooding Apparatus.

Before performing core flooding tests, leakage test should be applied to ensure measurements were conducted properly. For this purpose, pressurized gas was left in the closed apparatus for one or two days and any pressure drops, indication of leakage were recorded. Necessary adjustments were made until any drop in pressure was not observed. The same process was repeated after the core sample was replaced with another one and core holder was again connected to the apparatus to see if taking out and affixing of the chamber creates any leakage problem. Later on, water at 130 psig was injected to a core sample which is known to be impermeable with a confining pressure exceeding the inlet pressure by 5 bar to confirm that leakage does not occur between the core sample and rubber sleeve which wraps it at the corresponding pressure difference.

Amott cells were tested in the oven at 70 °C. The leakage occurred as the pressure in the amott cell increased was prevented glueing the plug which encloses the bottom of the cell with silicon. The top of the amott cells were closed with threaded lids (Figure 6.6).

Figure 6.6-The Amott Cell used in the study.

6.3 Core Preparation

The following general procedure was applied to prepare the core samples for Amott tests.

- Each core sample (if necessary) was flooded by toluene and then by methanol for cleaning.
- After the cleaning process, they were dried in the oven to evaporate remaining liquids inside the core samples.
- The core samples were saturated with the brine samples under vacuum and aged in the brine samples.
- After the aging process, the core samples were saturated with the oil samples using the core flooding apparatus.
- The core samples saturated both with oil and brine samples were aged in the oil samples prior to the imbibition experiments.

6.4 Results and Discussion

This section covers the detailed discussion of Amott tests of the core samples.

6.4.1 Core Sample 9/67

The core sample numbered as 9/67 was cleaned by flooding toluene and then by flooding methanol at a rate of 0.1 ml/min for 24 hours. The cleaning process was performed at ambient conditions. After the cleaning process, the core was dried at 105 °C for 18 hours. The dry core was saturated with formation brine sample (FW_4) (Table 4.2) under vacuum. The porosity was determined calculating the weight difference between wet and dry core. The wet core was aged in formation brine for 10 days. After that, it was flooded with the same brine to determine its permeability. The weight of the core sample was measured twice, before and after flooding, to check whether a significant change in the weight of the core sample occurred or not and thus to be sure about the correctness of the calculated porosities. The water saturated core was flooded with n-decane at a rate of 6 ml/min until water production ceased. Finally, the core sample was taken into chamber filled with the oil sample

used to saturate the core. The core was aged in the oil sample for 40 days at ambient conditions. Before the Amott cell including rock sample and the brine sample was taken into the oven, it was kept at ambient conditions for one day for silicon used to glue the plug to the bottom of the cell to harden.

Figure 6.7 shows the spontaneous imbibition into the core sample. At first, the experiment was conducted at ambient conditions for one day keeping the rock sample in the formation water sample. During this time, production of n-decane was not observed. After this one day of period, the rock sample was taken into oven at 70 °C and the rest of the experiment was performed at this temperature. Production of 8.8 percent of OIP was recorded while the rock sample was being kept in the formation water sample. The formation water sample was exchanged with the brine sample named as SSW*4S and additional 2 percent of OIP was observed to be produced. Exchanging the brine sample, SSW*4S with distilled water (DW) resulted in extra production of 1.5 percent of OIP. Similar production amounts were noted exchanging distilled water with new distilled water samples. Finally, formation water sample was tested again to observe if any further increment in recovery occurred. This time, production was observed but it was less than those of measured using the brine samples SSW*4S and DW.

That tendency of brine sample to wet the core and fill the pores is much higher than the nonpolar sample, n-decane was not reflected in the first day experiment can be attributed to high interfacial tension between water and n-decane, which is higher than 50 dynes/cm. Expansion factor and reduction in interfacial tension cause production of n-decane at a higher temperature 70 °C as distinct from the case at room temperature. The fact that interfacial tension between n-decane and brine decreases with reduction in brine salinity was reflected in this experiment as production occurred in parallel with expansion was higher when the brine sample, SSW*4S and distilled water were used in comparison to production occurred with formation brine utilization.

6.4.2 Core Sample 6

The core sample numbered as 6 was cleaned by flooding toluene and then by flooding methanol at a rate of 0.1 ml/min for 24 hours. The cleaning process was performed at ambient conditions. After the cleaning process, the core was dried at 105 °C for 18 hours. The dry core was saturated with formation brine sample (FW_4) (Table 4.2) under vacuum. The porosity was determined calculating the weight difference between wet and dry core. The wet core was aged in formation brine for 10 days. After that, it was flooded with the same brine to determine its permeability. The weight of the core sample was measured twice, before and after flooding, to check whether a significant change in the weight of the core sample occurred or not and thus to be sure about the correctness of the calculated porosities. The water saturated core was flooded with n-decane including 0.006 M stearic acid at a rate of 6 ml/min until water production ceased. Finally, the core sample was taken into chamber filled with the oil sample used to saturate the core. The core was aged in the oil sample for 40 days at ambient conditions. Before the Amott cell including rock sample and the brine sample was taken into the oven, it was kept at ambient conditions for one day for silicon used to glue the plug to the bottom of the cell to harden.

Figure 6.8 shows the spontaneous imbibition into the core sample. At first, the experiment was conducted at ambient conditions for one day keeping the rock sample in the formation water sample. During this time, production of n-decane was not observed. After this one day of period, the rock sample was taken into oven at 70 °C and the rest of the experiment was performed at this temperature. Production of 7.3 percent of OIP was recorded while the rock sample was being kept in the formation water sample. Then, the formation water sample was replaced with the brine sample named as SSW*4S. It seemed that very small amount of n-decane was produced. Although it was not clear, production of nearly 0.4 percent of OIP was recorded. N-decane production was not observed changing the brine sample, SSW*4S with distilled water.

Nil production of n-decane during the first day of experiment was thought to be due to lower water wetness because of the existence of stearic acid and high interfacial tension between brine sample and n-decane. The contribution of expansion to n-decane production can be seen after the sample was taken into the oven. That exchanging brine sample with sulphate reach brine, SSW*4S and distilled water did not contribute to production even these samples lowered the interfacial tension might be due to lower water wetness of the rock sample because of existence of stearic acid that increase the oil wettability.

6.4.3 Core Sample K16 (H1)

The core labeled as K16 (H1) was cleaned with toluene injected at a rate of 0.1 ml/min for one day then it was cleaned with 4 pore volumes of methanol injected at a rate of 0.1 ml/min. After the cleaning process, it was dried at 90 °C for one day. The core was saturated with the brine sample the salinity of which was 106.5 g/L (FW_3) (Table 4.2) under vacuum and aged in the brine sample for 7 days. It was flooded with oil sample K (Table 4.3) at a rate of 6 ml/min and 5 ml of water production was observed with 3 psig of inlet pressure. Then, the injection rate was increased to 10 ml/min and 1 ml of water production was observed with 5 psig of inlet pressure. Final oil saturation was estimated as 40 percent. The core sample being wrapped in teflon was aged in the oil sample for 40 days at ambient conditions.

Figure 6.9 shows the spontaneous imbibition into the core sample at ambient conditions. Nearly 21 percent of OIP was produced while the sample was kept in formation water sample in the Amott cell. Oil production was not observed after exchanging the formation brine sample with distilled water and after exchanging distilled water with sulfate rich water, SW*4SO4. Finally, liquid detergent dissolved in pure water was tested. Notable production, 12 percent of OIP, was observed as a result.

It is possible that distilled water and sulfate rich water, SW*4SO4 did not lower (actually increase) the interfacial tension similar to the case seen in Figure 5.1 which

was drawn for Bozhuyuk oil the base number of which was much higher than acid number like Camurlu heavy oil. That the effectiveness of sulfate ions and divalent cations in wettability alteration was not reflected on the graph might be due to increase in interfacial tension and insufficient diffusion of surface active ions into rock sample. Addition of liquid detergent into distilled water lowered the interfacial tension measured for pure water to nearly its half value. Decrease in interfacial tension with the addition of liquid detergent was reflected on the graph with 12 percent increase in oil recovery. Imbibition of the formation brine halted due to interfacial tension around the core sample again became active with decrease in the tension.

6.4.4 Core Sample K1 (H1)

The core labeled as K1 (H1) was cleaned with toluene injected at a rate of 0.1 ml/min for one day then it was cleaned with 4 pore volumes of methanol injected at a rate of 0.1 ml/min. After the cleaning process, it was dried at 90 °C for one day. The core was saturated with the brine sample the salinity of which was 106.5 g/L (FW_3) (Table 4.2) under vacuum and aged in the brine sample for 7 days. After the aging process, it was flooded with the oil sample K (Table 4.3) at a rate of 6 ml/min. 2.5 ml of water production was observed and inlet pressure increased up to 45 psig. Final oil saturation was estimated as 28 percent. The core sample being wrapped in teflon was aged in the oil sample for 40 days at ambient conditions.

Figure 6.10 shows the spontaneous imbibition into the core sample at ambient conditions. Oil production was not observed during testing of formation brine sample, distilled water and sulfated brine, SW*4SO4. Finally, liquid detergent dissolved in pure water was tested and recovery of 4 percent of OIP was observed.

The fluids used to saturate the core sample were the same fluids used to saturate the core sample K16 (H1). In spite of 21 percent of OIP production with utilization of formation brine sample for the core sample K16 (H1), nil production was observed using the same brine for the core sample K1 (H1) which has lower permeability and

porosity. Narrower pore structure of the core sample was possibly the reason of such observation. Gravity forces might not be enough to carry out the oil through such narrow pore bodies. The effect of reducing the interfacial tension using liquid detergent can be seen with production of 4 percent of OIP. Similar to situation seen in Figure 6.9, exchanging the formation brine sample with distilled water and exchanging the distilled water with sulfated brine did not result in any oil recovery, an indication of interfacial tensions not being reduced and similarly, surface active ions in sulfated water did not enhance oil recovery in this case.

6.4.5 Core Sample A7

The core sample labeled as A-7 was saturated with distilled water under vacuum. The porosity was calculated from the weight difference between dry and wet cores. The sample was aged in distilled water for 10 days. After 10 days of aging period, the core sample was saturated with toluene at an injection rate of 10 ml/min. During injection process, increase in inlet pressure was not observed due to the fact that the sample is highly permeable. Total water production was 9 ml. The core sample was aged in toluene for 15 days at ambient conditions.

Figure 6.11 shows the spontaneous imbibition into the core sample at ambient conditions. At first, distilled water was tested and recovery of 4.4 percent of OIP was observed. Changing distilled water with sulfated brine, a little amount of toluene (0.4 percent of OIP) was observed to be produced. Finally, liquid detergent dissolved in distilled water was tested and significant enhancement in recovery was observed with extra production of 14 percent of OIP.

With utilization of distilled water as a saturation fluid, possible enhancement in oil recovery due to reduction in interfacial tension was eliminated. Almost nil production occurred exchanging distilled water in amott cell with sulfated brine. It can be deduced that surface active ions in sulfated water did not contribute to improvement in oil recovery. On the other hand, reduction in interfacial tension

nearly two times with liquid detergent utilization results in significant increase in oil recovery.

6.4.6 Core Sample A8

The core sample labeled as A-8 was saturated with 200 g/L NaCl solution. After aged in the brine sample for 7 days, the core sample was flooded with toluene at incremental rates. Toluene was injected at rates of 0.4 ml/min, 1 ml/min, 2 ml/min, 4 ml/min and 8 ml/min for 33 minutes, 7 minutes, 5 minutes, 2 minutes and 9 minutes, respectively. Observed production was 4 ml when the injection rate was 0.4 ml/min, around 1 ml when the injection rates were 1 ml/min, 2 ml/min and 4 ml/min and 2 ml when the injection rate was 8 ml/min. Total production being 9 ml was same with the total water production observed for the core sample labeled as A7 which was flooded at a constant injection rate, 10 ml/min. In the last step, the core sample was aged in toluene for 14 days at ambient conditions.

Figure 6.12 shows the spontaneous imbibition into the core sample at ambient conditions. Nearly, 6 percent of OIP was produced while rock sample was being kept in the brine. Then, the brine sample was changed with distilled water and extra 3 percent of OIP was produced.

Proving increase in recovery using surfactant liquid detergent, the aim of this experiment was to observe the improvement in oil recovery by reducing the interfacial tension between brine and oil sample with decrease in salinity. Decrease in salinity was not beneficial for the core samples saturated with oil sample J and for the core samples saturated with n-decane, the effect was not clear due to the expansion resulted from heating of the Amott cell in the oven after the replacement process conducted at ambient conditions. This time, the experiment was fully conducted at ambient conditions.

Reduction in interfacial tension between water and toluene with decrease in the salinity was proved with measurements conducted with ring tensiometer. Interfacial tension between the brine and toluene was measured as 32 dynes/cm while the

interfacial tension between distilled water and toluene was measured as 26 dynes/cm. Reduction in interfacial tension reflected in the measurements. Changing the brine surrounding the rock sample with pure water resulted in decrease in interfacial tension around the core sample and thus extra 3 percent of OIP was produced. Unlike other formation brines, the brine sample used in this experiment was lack of divalent cations, thus the tendency of making the rock surface more water-wet with these cations was eliminated.

6.4.7 Core Sample BS

Berea sandstone was cleaned by injecting toluene and then by injecting methanol at a rate of 0.1 ml/min for 24 hours. The cleaning processes were performed at ambient conditions. After the cleaning process, the core was dried at 90 °C for two days. The dry core was saturated with the formation brine sample, FW_3 (Table 4.2) under vacuum. The porosity was determined calculating the weight difference between wet and dry core. The wet core was aged in the formation brine for 10 days. After that, it was flooded with the same brine to determine its permeability and to ensure that there is not a significant change in the weight of the core. The water saturated core was flooded with oil sample H (Table 4.3) at a rate of 6 ml/min until water production ceased. Final water saturation was 0.31 as fraction. More water could be produced increasing the inlet pressure, but this was not performed not to disturb clay content. Finally, the core was wrapped up with teflon to avoid asphaltene precipitation around it and taken into a chamber filled with the oil sample used to saturate the core. The core was aged in the oil for 40 days at around 25 °C.

Figure 6.13 shows the amount of oil produced in Amott cell with respect to time for Berea sandstone. At the beginning, production rate was high but later on it approached to zero and cumulative production stabilized. Final cumulative production was very low compared to initial oil in place, which indicates low water wettability. Such low water wettability is thought to be achieved with the addition of Batı Raman heavy oil which has high asphaltene concentration, high base number, on the other hand low acid number and with the addition of non-polar liquid, n-

decane for decreasing the solubility of asphaltenes in the mixture. Figure 6.14 shows the oil bubbles beneath the oil and brine interface. Some portions of polar components can be separated from the oil sample and migrated to the water phase as solubility of them can be higher in the water phase. Such condition is seen in the figure and it can be assumed that it contributes to increase in oil wettability.

Formation brine in the Amott cell was replaced with low saline water obtained by diluting the formation water around 20 times. The core sample was kept in this low saline water for about 30 days. As can be seen from figure, reducing brine salinity did not increase the cumulative production (Figure 6.13).

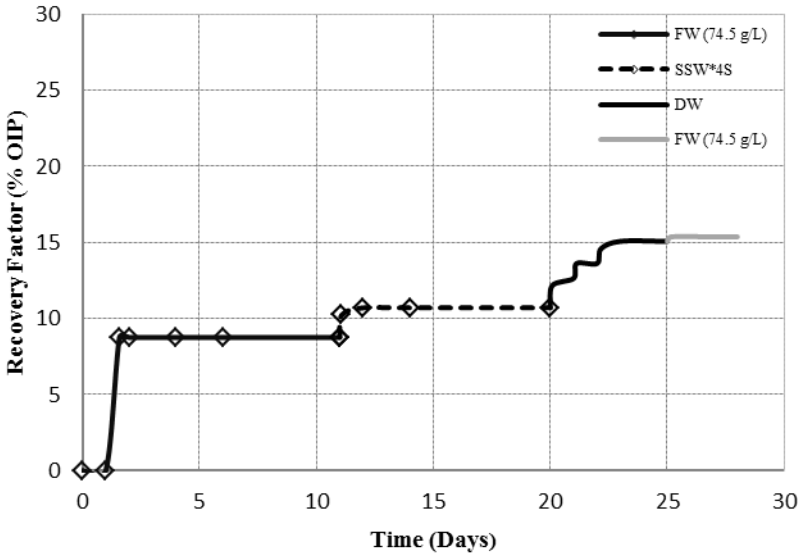

Figure 6.7- Imbibition into the core sample numbered as 9/67.

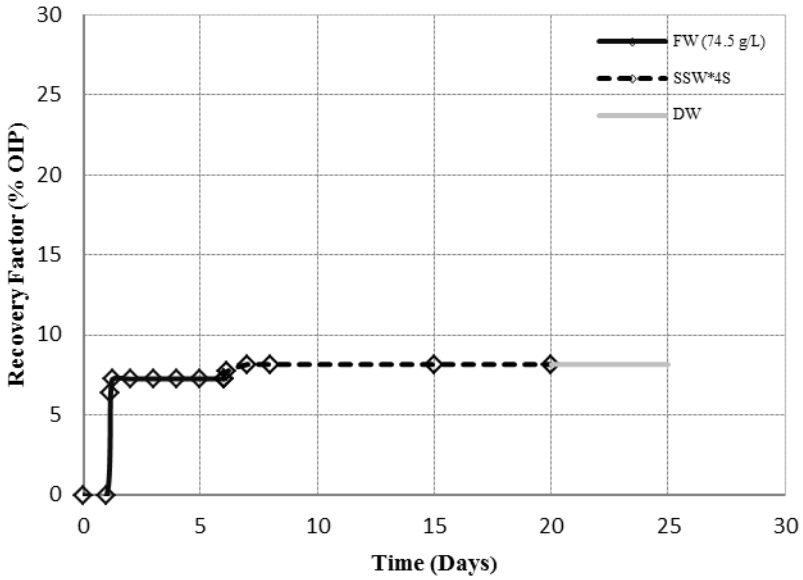

Figure 6.8- Imbibition into the core sample numbered as 6.

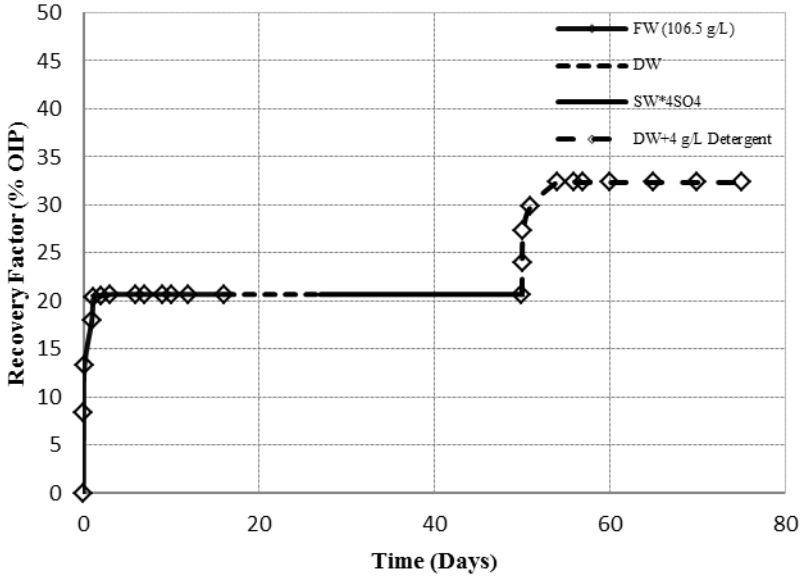

Figure 6.9- Imbibition into the core sample labeled as K16 (H1).

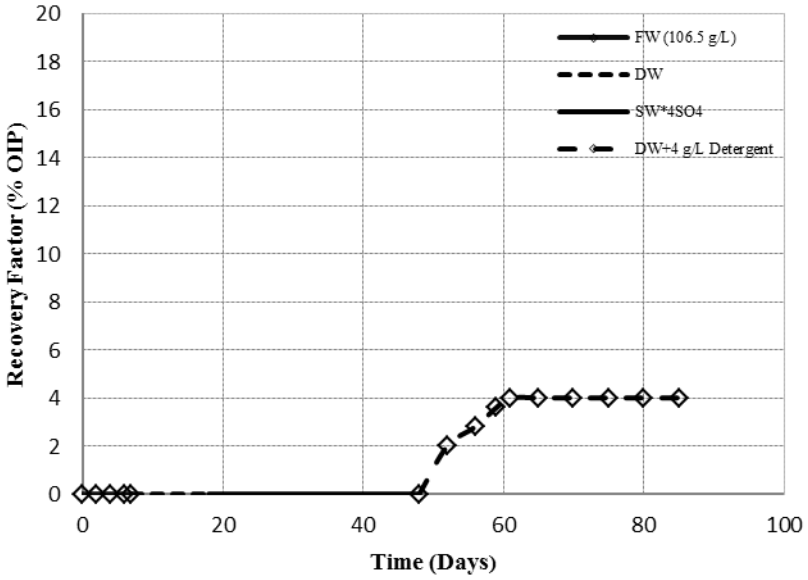

Figure 6.10- Imbibition into the core sample labeled as K1 (H1).

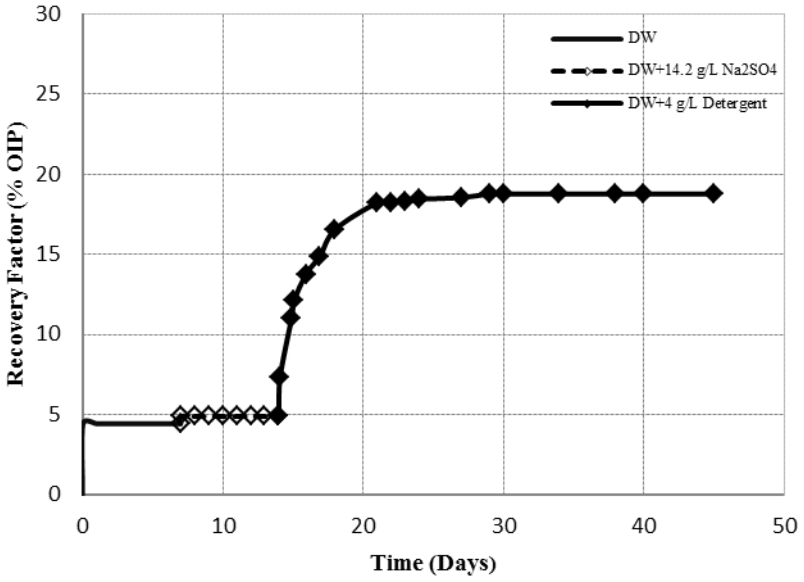

Figure 6.11- Imbibition into the core sample labeled as A7.

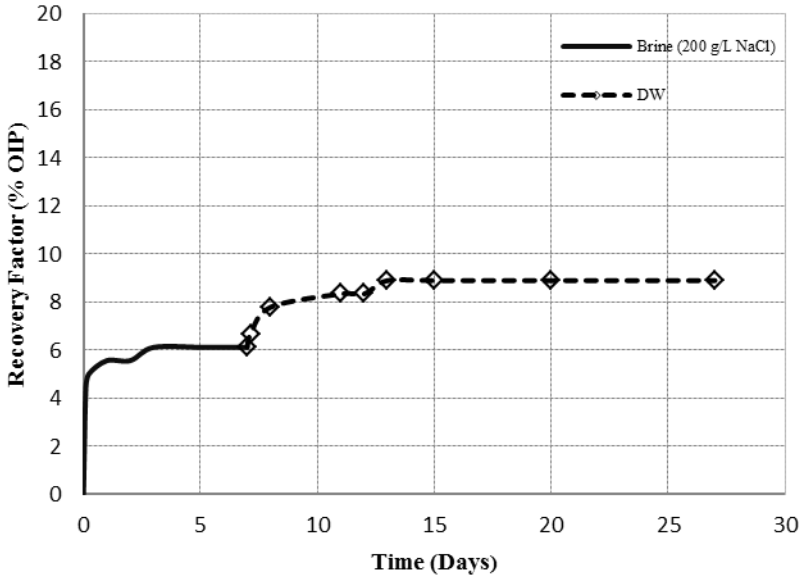

Figure 6.12- Imbibition into the core sample labeled as A8.

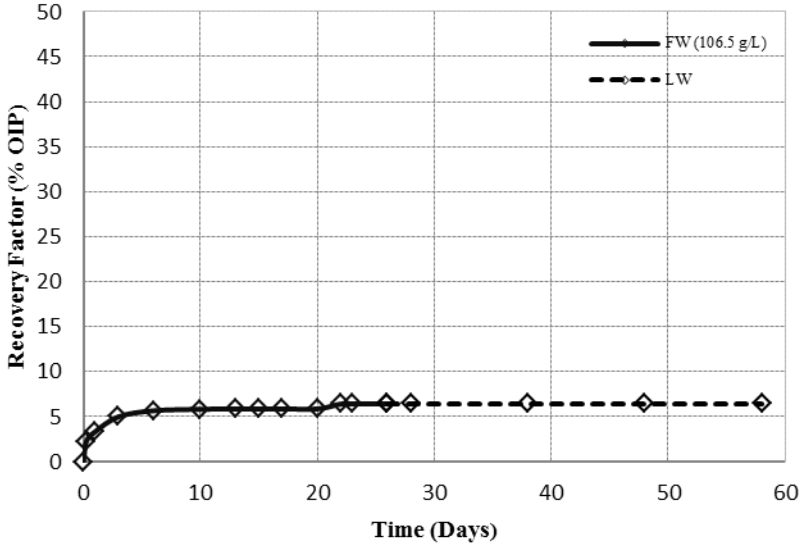

Figure 6.13- Imbibition into the core sample labeled as BS.

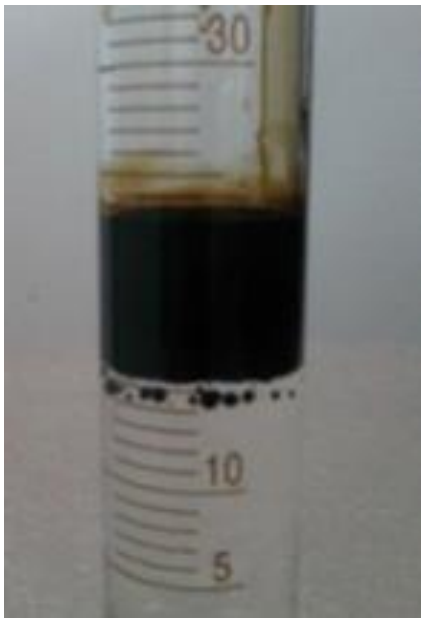

Figure 6.14- Oil particles suspended beneath the oil/brine interface.

CHAPTER 7

FLOW VISUALIZATION WITH VIDEO CAMERA

7.1 Materials

The rock sample is a highly permeable limestone which includes small amounts of quartz and feldspar apart from the calcite mineral. Petrography analysis did not indicate any fractures and water soluble components in the sample.

Oil samples L and K (Table 4.3), toluene, brine sample FW_1 (Table 4.2) and distilled water were used to saturate the core samples.

FW_1, distilled water and liquid detergent solution were injected to recover oil.

The liquid detergent was composed of % 5 – 15 anionic surfactant, <% 5 nonionic surfactant and preservatives which are benzisothiazolione, phenoxyethanol and geraniol.

7.2 Experimental Setup

The apparatuses used in this study were prepared utilizing the information about preparation of the micromodel shown in the visualization study of Khan et al. [56].

In the first part of the study, the rock slice was prepared by cutting the rock sample with diamond saw. Surface of the slice was smoothened with diamond abrasive disc and horizontal disc. The sides of the slice were enclosed with a polyamide material and the space between the slice and polyamide material was filled with epoxy. The upper and bottom of the slice were enclosed with tempered glasses attached to the material with silicon. Two more tempered glasses were used to compress the glass on

the surface of the slice with bolts and loafs. Connectors were attached to the inlet and outlet of the model (Figure 7.1).

In the second part of the study, the rock slice used in the visualization study was prepared by cutting the rock sample with diamond saw. Before the slice was inserted into a mold filled with epoxy (Figure 7.2), it was wrapped with cement to prevent intrusion of epoxy into the slice. It was kept in epoxy for one day until the epoxy was completely hardened. The voids at the inlet and outlet sections were created with a milling machine (Figure 7.3). Surface of the rock slice was smoothened with a band emery machine (Figure 7.4). Then, a tempered glass was attached to the top surface with epoxy. Two more tempered glasses were used to compress the glass on the surface of the slice with bolts and loafs. Connectors were attached to the inlet and outlet of the model (Figure 7.5).

Width, length and height of the slices are 2 cm, 5 cm and 1 cm respectively.

Movement of oil and water at the top surface was filmed with a video camera.

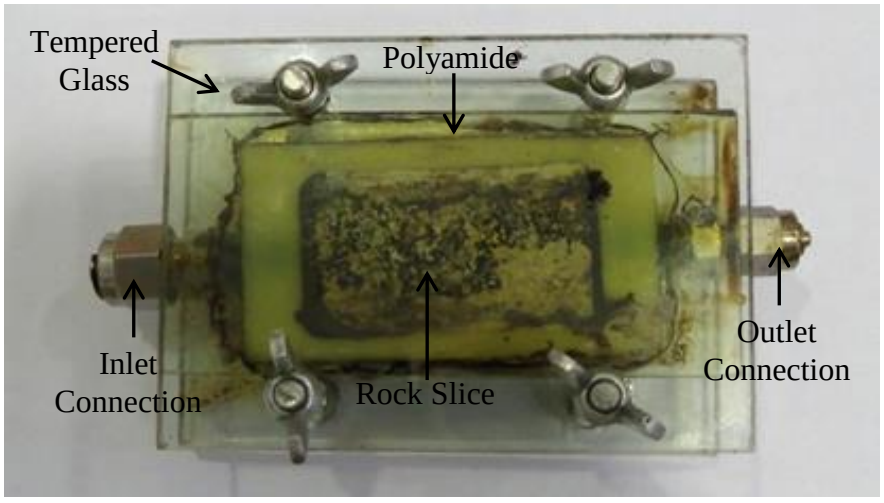

Figure 7.1- Top view of the slice 1.

Figure 7.2- The mold into which the rock slice was inserted.

Figure 7.3- The milling machine used for creating the voids.

Figure 7.4- The band emery machine used for smoothing the surface of the rock slice.

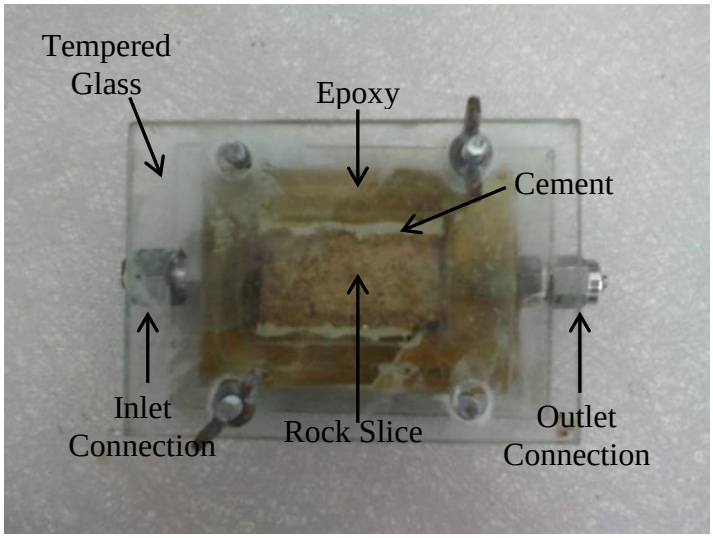

Figure 7.5- Top view of the slice 2.

7.3 Procedure, Results and Discussion

In the first part of the experiment, flow types were tried to be determined under different wetting conditions.

During the oil recovery process, it is expected to see water in the center of pore bodies if the rock is oil-wet. Figure 7.6 and Figure 7.7 show the movement of oil (oil sample K) (Table 4.3) with the appearance of water phase (distilled water). Water appears as a point inside a region previously swept with oil. Then, the circle enlarges up to a point and the process causes the removal of oil. Water did not contact with rock surface. The rock was thought to be oil-wet. The injection rate was 0.5 ml/min.

Figure 7.8 shows the movement of oil under the case the rock is water wet. Rupturing of the oil phase at the narrow section can be observed. Toluene was used as the oil phase. A small amount of heavy oil was added to toluene to change its color for differentiation with water.

Figure 7.9 and Figure 7.10 show captured images during oil (oil sample L) (Table 4.3) flooding of the slice which was first saturated with water (distilled water) under vacuum. Oil was injected at a rate of 6 ml/min. Captured water bodies were observed as oil moved more rapidly through highly permeable pathways. Capillarity-controlled flow of these captured bodies was observed. Figure 7.10 shows the movement of meniscus water from one pore to a nearby pore through a narrower section, which can be regarded as a jump process and Figure 7.9 shows the choke off event, rupturing of the non-wetting fluid which is water in this case at the narrow pore throat.

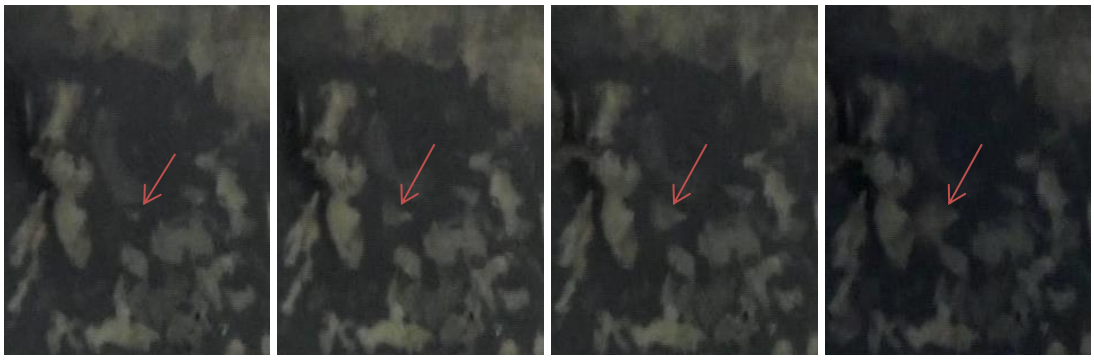

Figure 7.6- Water flooding in an oil-wet rock. Water bubble enlarges inside the oil phase.

Figure 7.7- Enlargement of the water bubble inside the oil phase.

Figure 7.8- Rupturing of the oil phase during water flooding in a water-wet rock.

Figure 7.9- Choke off process. Oil displaces water.

Figure 7.10- Jump process. Oil displaces water.

In the second part of the experiment, the slice was saturated with a brine sample the salinity of which was 213 g/l (Table 4.2). It was aged in the brine for 5 days. After aging, toluene was injected.

Figures 7.11 – 7.21 show the top view during oil flooding of the rock slice initially saturated with the brine sample. First, toluene was injected at a rate of 0.11 ml/min for one hour. Then, the injection rate was increased gradually starting from 0.33 ml/min upto 8.8 ml/min. Toluene was injected at rates of 0.33 ml/min, 0.99 ml/min,

3.1 ml/min, 6.7 ml/min and 8.8 ml/min for 20 minutes, 6 minutes, 2.5 minutes, 1 minute and 1 minute respectively.

The flow of toluene should be considered at two different conditions, before breakthrough and after breakthrough. Before breakthrough, movement of toluene was hampered with surface and interfacial tensions being more severe at narrow sections. As the movement of toluene ceases, pressure is built up with continuous injection. Then, pressure comes to a point at which it overcomes the tensions and the trapped toluene starts to move following possible easiest (widest) pathway. This process continues until breakthrough and because of preference to flow through wider sections, smaller pores remains unswept and some of the brine remained in this area will form the irreducible saturation.

Breakthrough occurred during injection at slow rate, 0.11 ml/min. After breakthrough, the swept area did not change with this slow rate. Different from the case before breakthrough, pressure did not build up as flow pathway of toluene was open-ended. The aim for increasing the injection rate was to increase pressure in oil phase for viscous forces to become more effective. The swept area was not changed increasing the injection rate to 0.33ml/min and then to 0.99 ml/min. But, some portion of the brine in the upper corner near to the entrance was flooded by increasing the flowrate to 3.1 ml/min. It should be pointed out that the swept portion was close to the entrance was because of that highest pressure occurred at the entrance during flooding. Further increasing the injection rate to 6.7 ml/min resulted in increase in swept area in this zone. At the highest injection rate, 8.8 ml/min, more portions were swept. This time, lower sections were flooded.

Another point to consider during toluene flooding was rupturing of the toluene at narrow section indicated with Figure 7.22. Because of continuous injection, pressure builds up at the narrow section where interface is more resistant to flow. Increased pressure is not sufficient for meniscus to flow. Rather, swelling occurs rupturing the meniscus. This swelling and rupturing was a continuous process ended when the

accumulating toluene completely filled the pathway between this narrow section and outlet.

After the saturation process, the liquids locating in the voids at the inlet and outlet sections were taken out and these voids were filled with toluene. The entrance and exit of the apparatus were closed with blind plugs. The rock slice being in contact with toluene was aged in this closed apparatus.

Figure 7.23 shows the view after 10 days aging. It is seen that toluene was replaced with brine in some areas during the period of aging. This movement is clear in the lower section which was able to be flooded with the highest injection rate, 8.8 ml/min, in other words, with possibly highest pressure after breakthrough. That the wetting phase, in this case brine, tends to occupy smaller pores and moves the non-wetting phase in these pores to possible larger pores can be observable as the narrow portions swept by toluene with high pressure was filled with brine and toluene was moved to the middle part near to exit during aging period.

After aging, formation brine was injected at a rate of 0.05 ml/min to recover toluene. Production or movement of toluene was not observed during the injection of formation brine for 4.5 hours. Nil production can be attributed to wide openings occurred during smoothing rock surface. It is possible that toluene flooded mainly the area between surface and glass as the pores at the surface are larger than the pores in the deeper parts. Higher section being flooded with toluene and deeper section being filled with brine, the injected brine possibly followed the pathways in the deeper section and bypassed the higher section filled with toluene (Figure 7.23 – 7.26).

Secondary flooding was performed with distilled water which was used to obtain lower interfacial tension compared tension between formation brine and toluene. The recovery was not observed during 30 minutes of injection, which can be attributed to insufficient decrease in salinity of the brine (Figure 7.28). The effect of reducing interfacial tension can be seen from Figure 7.29 taken after 1 hour of injection. It

seems that the toluene in the middle part and lower part near to the exit was flooded with distilled water. Further removal of toluene can be seen from Figures 7.30, 7.31, and 7.32 after 1.5, 3 and 5 hours of injection.

Finally, liquid detergent dissolved in distilled water was injected to observe any further recovery with more reduction in interfacial tension. Figures 7.33 – 7.37 show the captured views before and during the injection of liquid detergent solution. As can be seen from Figure 7.34, the effect of utilization of surfactant was not clear after 30 minutes of injection, which might be due to insufficient mixing of the solution with the brine sample previously located in the rock slice. The recovery was observable in Figure 7.35 showing the view after 60 minutes of injection. It is seen from Figure 7.37 that more toluene was produced and little amount of toluene was left in the rock after 3 hours of injection.

This study shows the importance of reducing interfacial tension with decrease in salinity of the brine on oil recovery. The rock slice having wider openings on the surface compared to below parts can be thought as an example of case in which oil is located in larger pores such as vugular pores while the brine flooding in smaller pores around it.

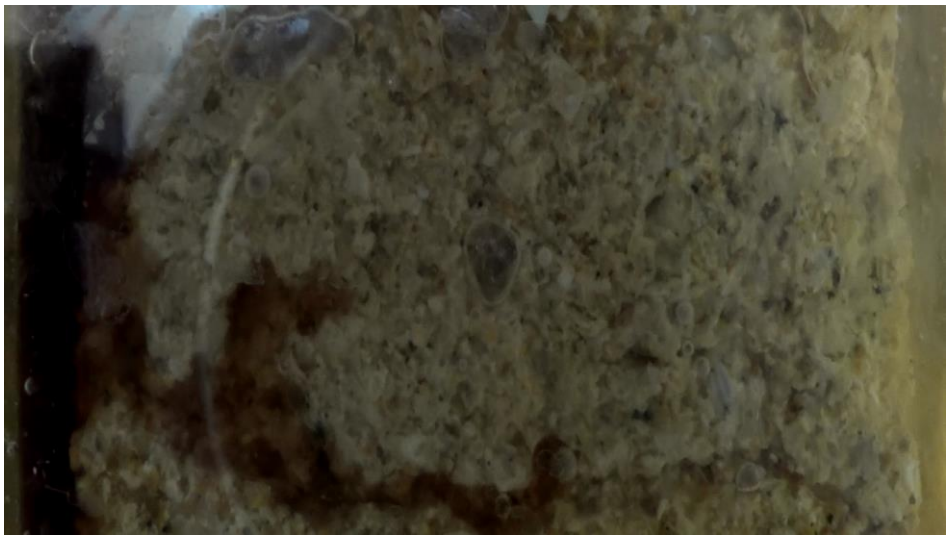

Figure 7.11- Top view after 2.50 minutes of injection of toluene at a rate of 6.7 ml/hour.

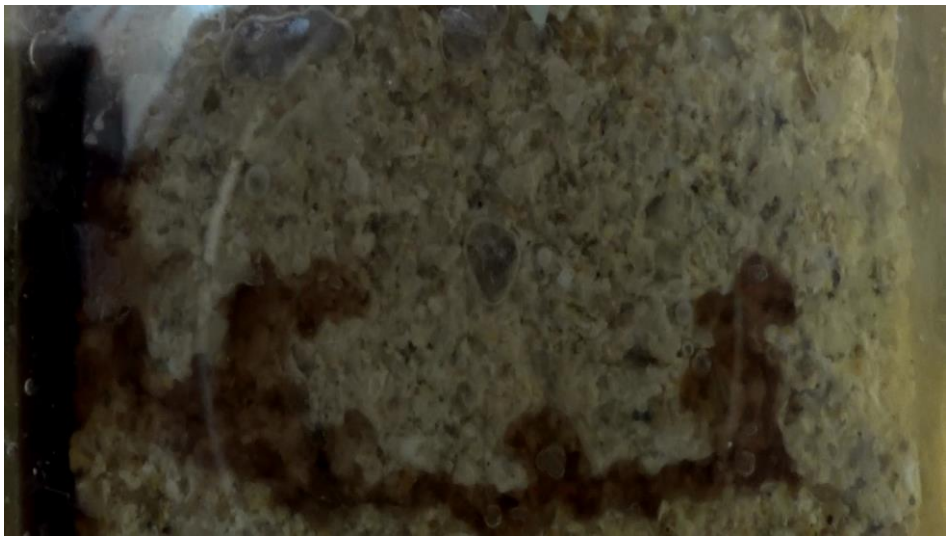

Figure 7.12- Top view after 4 minutes of injection of toluene at a rate of 6.7 ml/hour.

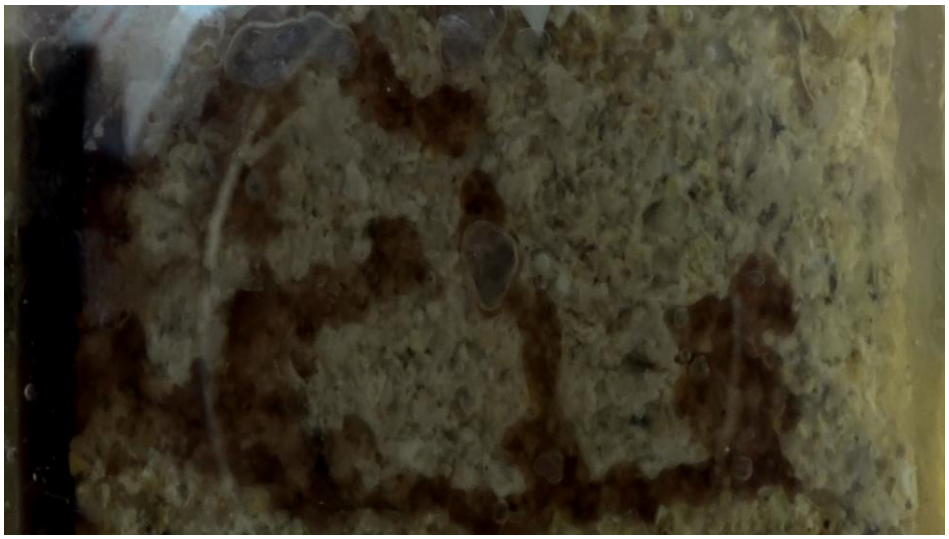

Figure 7.13- Top view after 5 minutes of injection of toluene at a rate of 6.7 ml/hour.

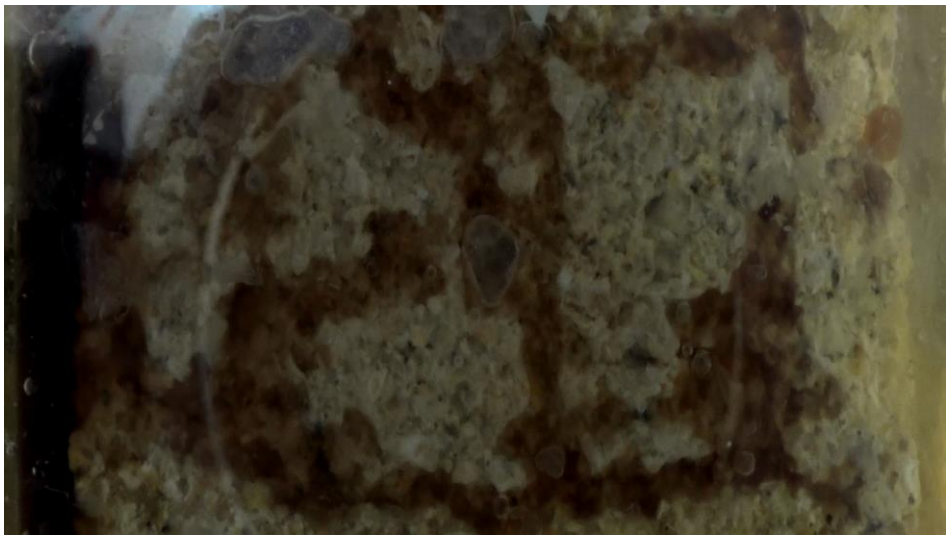

Figure 7.14- Top view after 6 minutes of injection of toluene at a rate of 6.7 ml/hour.

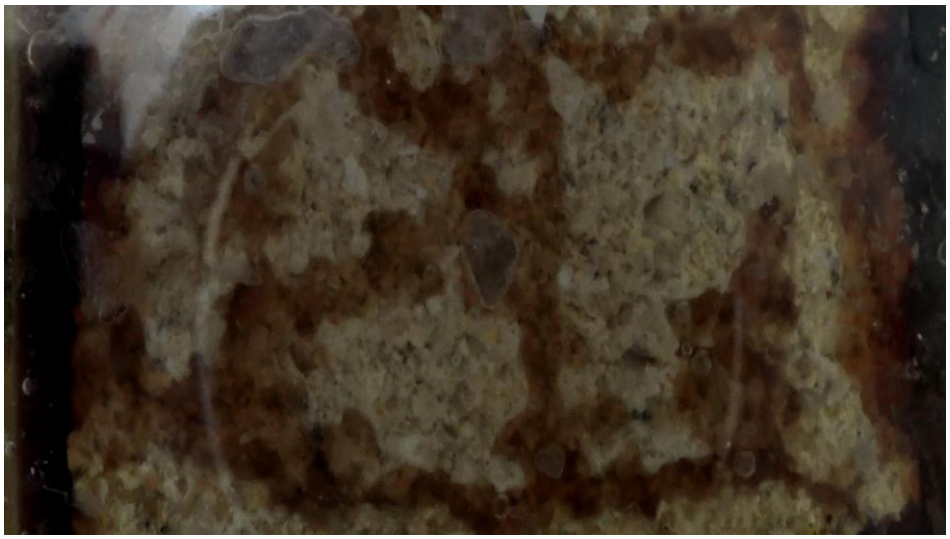

Figure 7.15- Top view after 30 minutes of injection of toluene at a rate of 6.7 ml/hour.

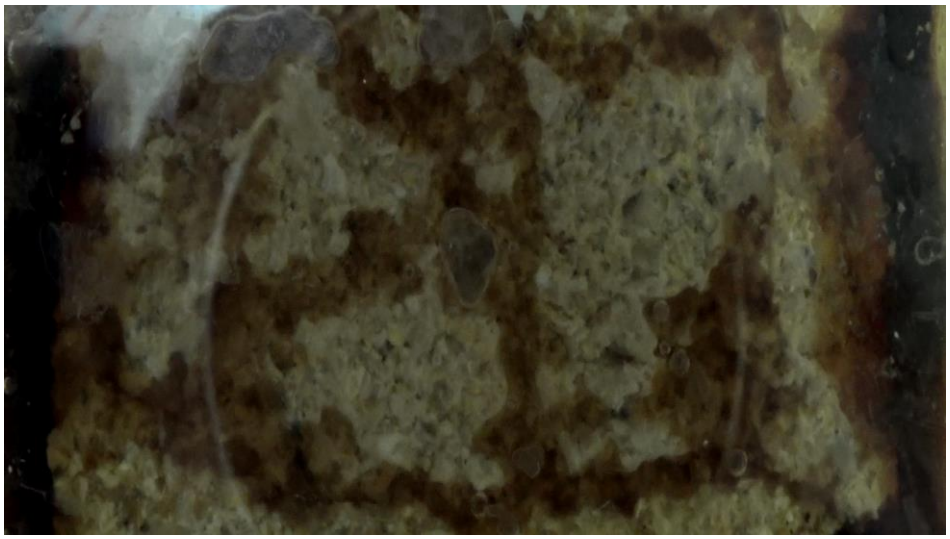

Figure 7.16- Top view after 60 minutes of injection of toluene at a rate of 6.7 ml/hour.

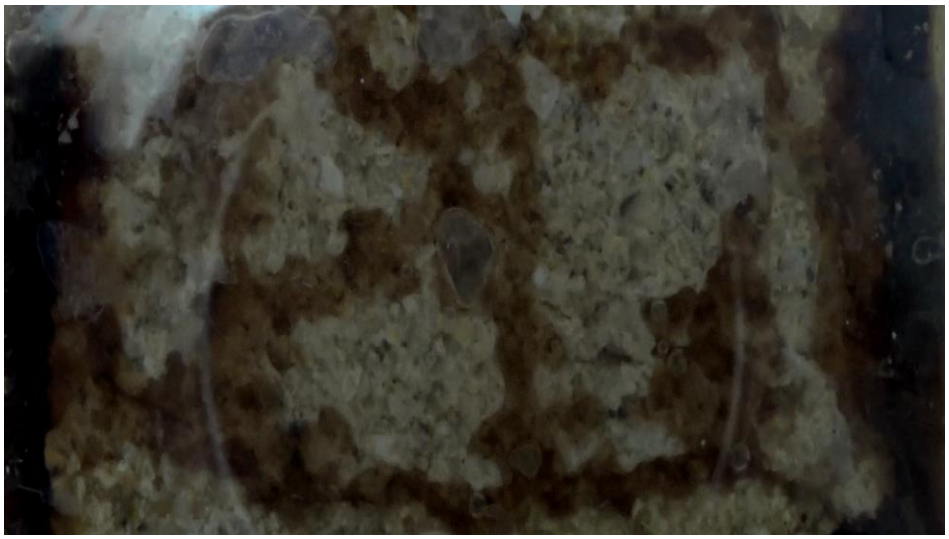

Figure 7.17- Top view after 20 minutes of injection of toluene at a rate of 0.33 ml/min.

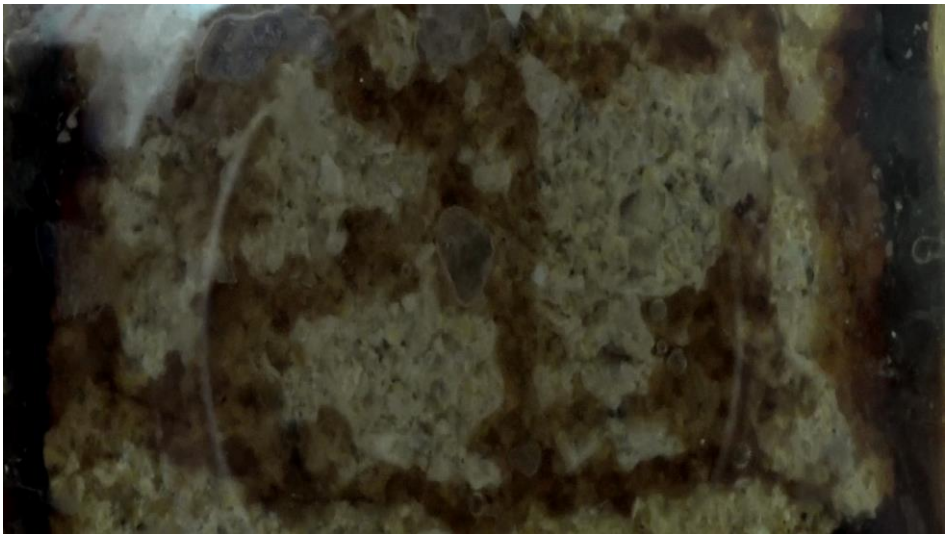

Figure 7.18- Top view after 6 minutes of injection of toluene at a rate of 0.99 ml/min.

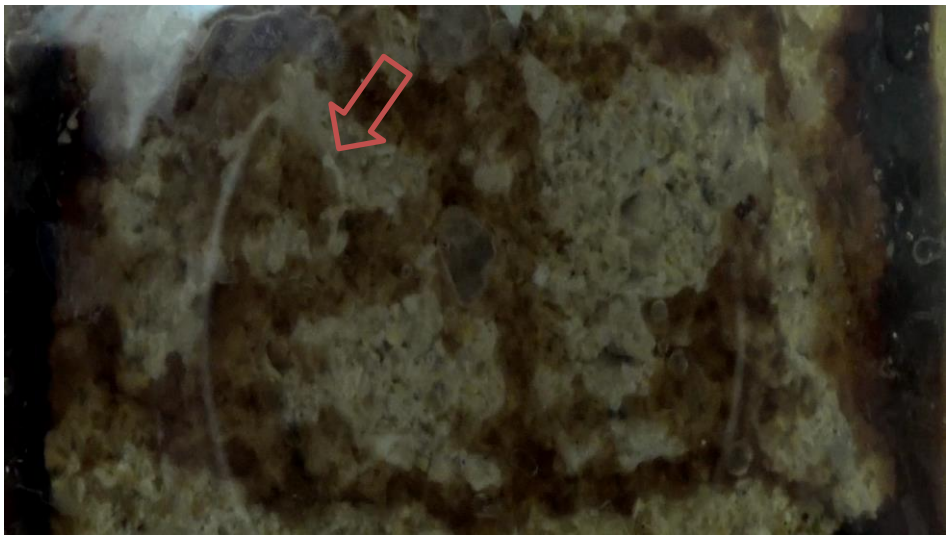

Figure 7.19- Top view after 2.5 minutes of injection of toluene at a rate of 3.1 ml/min.

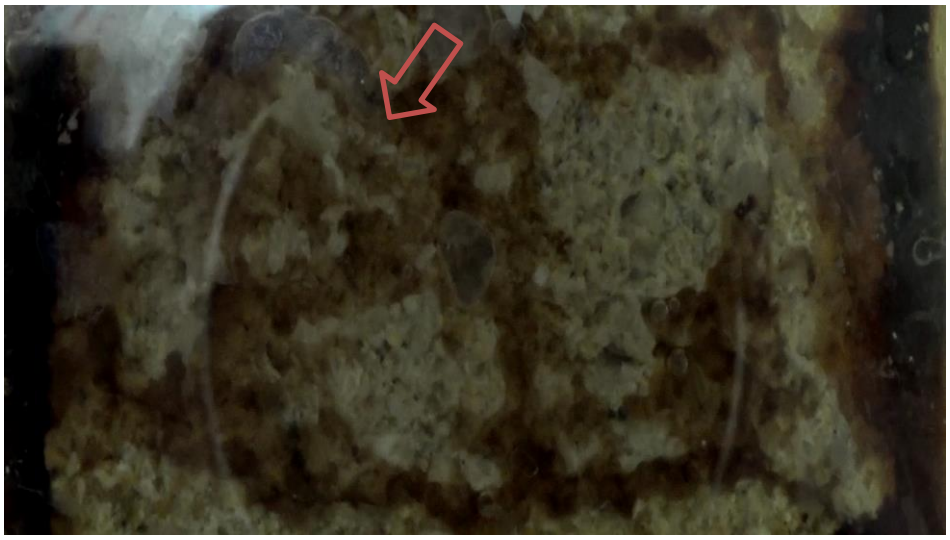

Figure 7.20- Top view after 1 minute of injection of toluene at a rate of 6.7 ml/min.

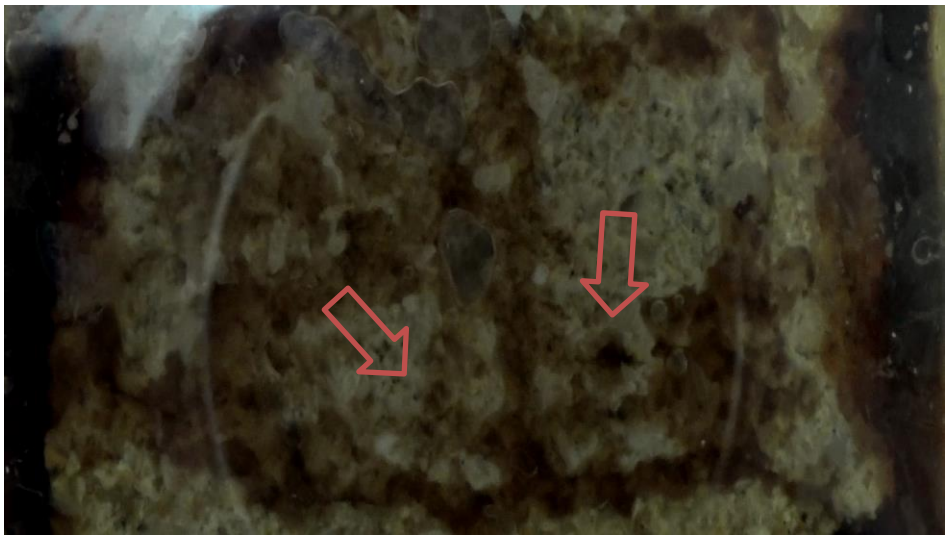

Figure 7.21- Top view after 1 minute of injection of toluene at a rate of 8.8 ml/min.

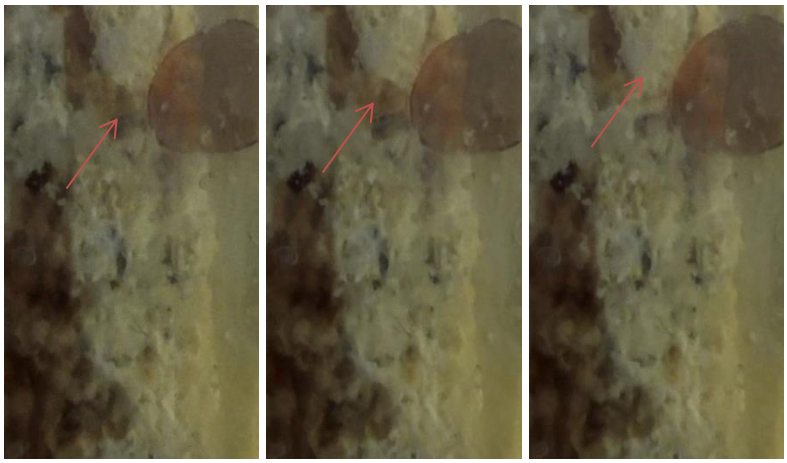

Figure 7.22- Rupturing of the toluene at the narrow section.

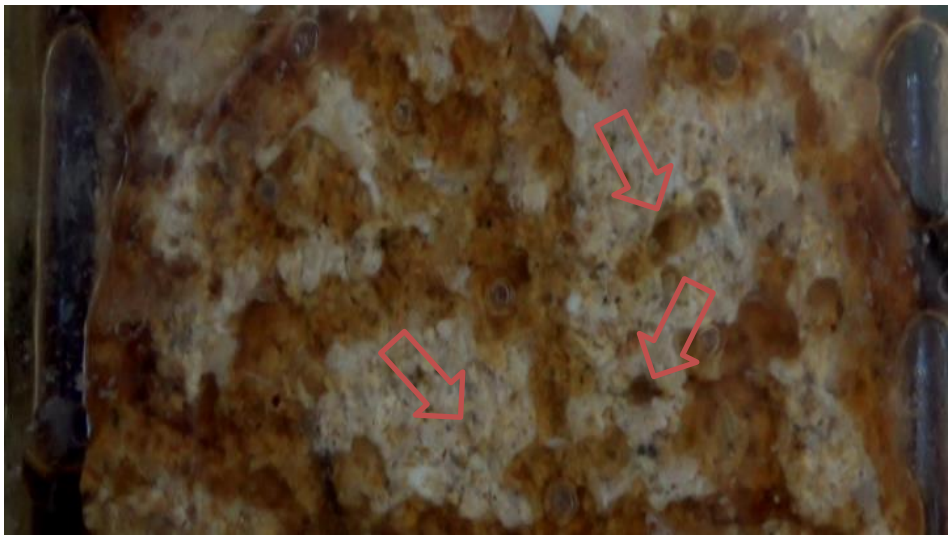

Figure 7.23- Top view after 10 days of aging in toluene.

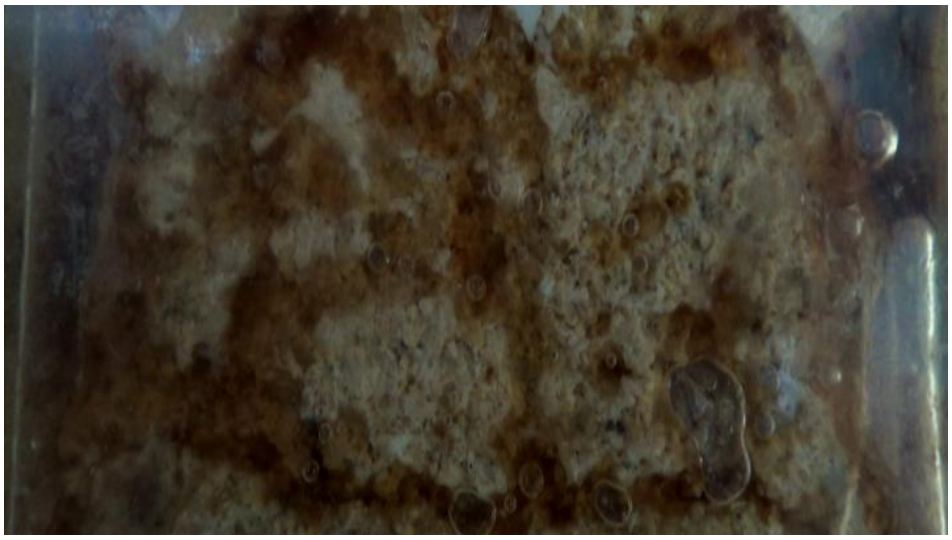

Figure 7.24- Top view after 60 minutes of injection of the brine sample at a rate of 0.05 ml/min.

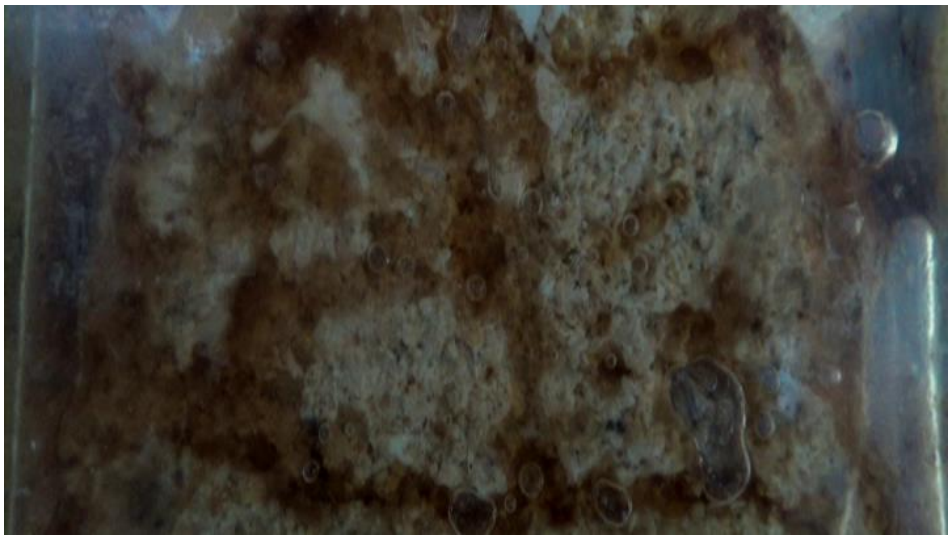

Figure 7.25- Top view after 120 minutes of injection of the brine sample at a rate of 0.05 ml/min.

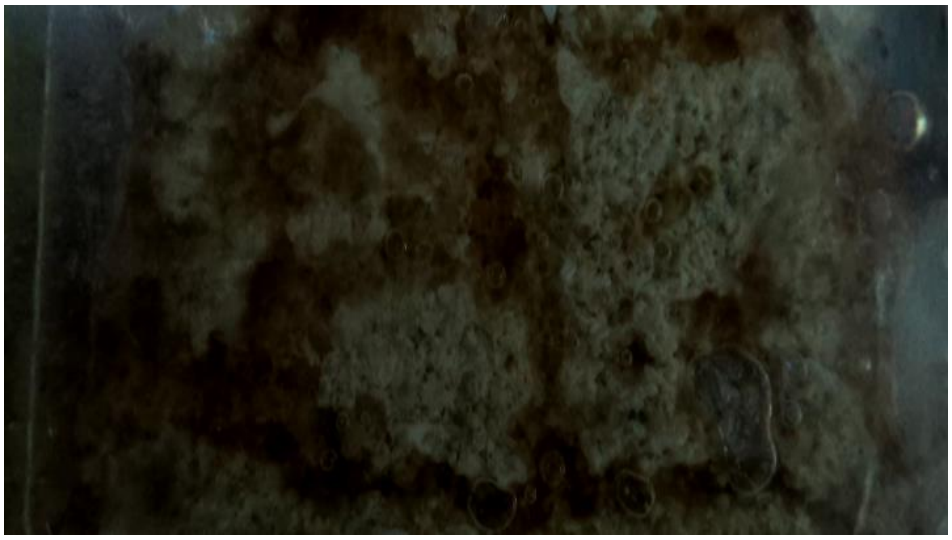

Figure 7.26- Top view after 4.5 hours of injection of the brine sample at a rate of 0.05 ml/min.

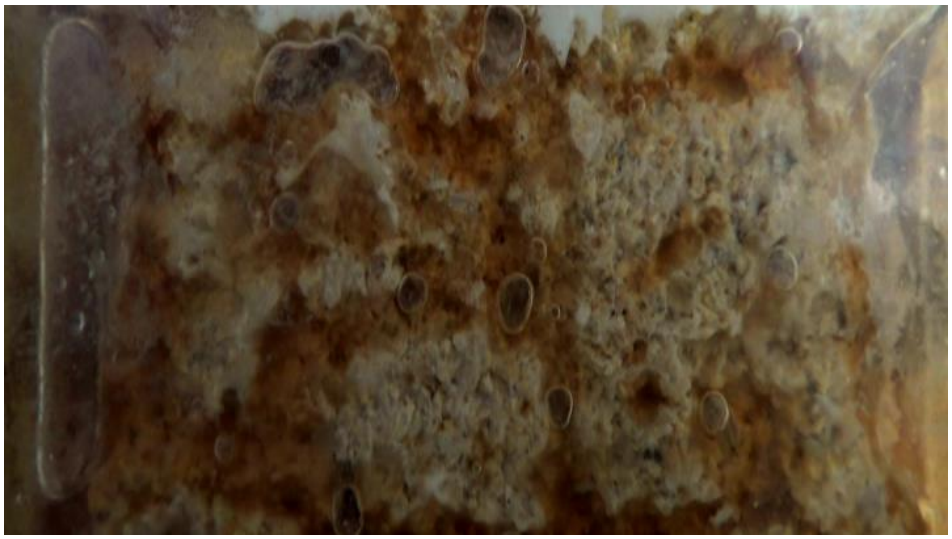

Figure 7.27- Top view before injection of distilled water.

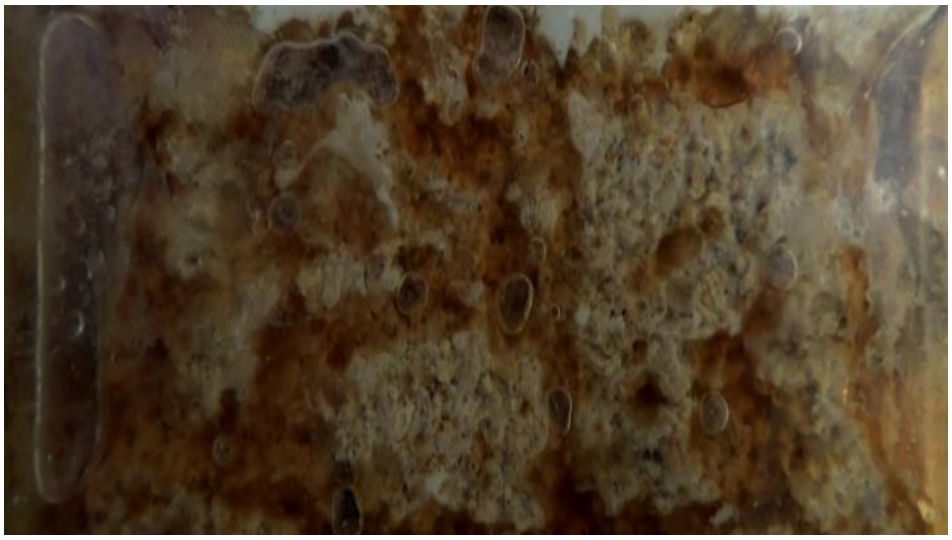

Figure 7.28- Top view after 30 minutes of injection of distilled water at a rate of 0.05 ml/min.

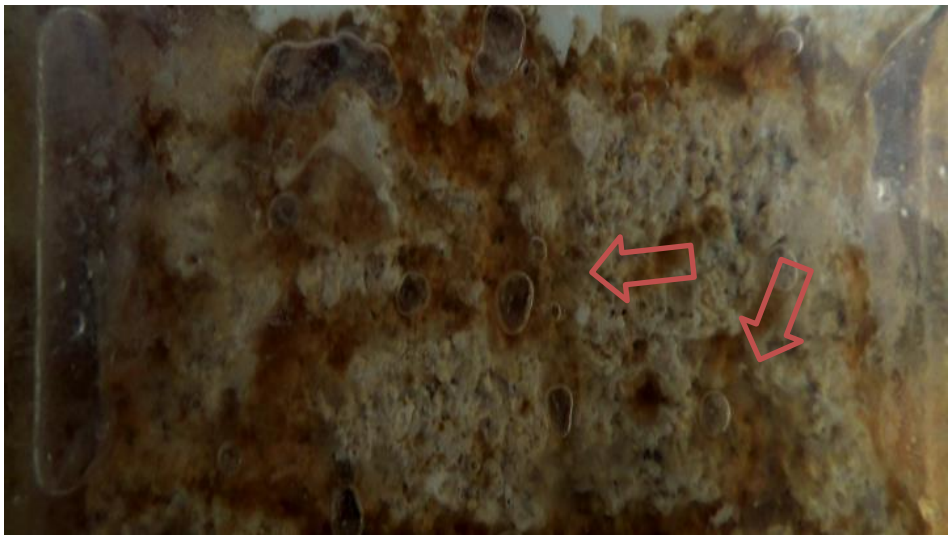

Figure 7.29- Top view after 60 minutes of injection of distilled water at a rate of 0.05 ml/min.

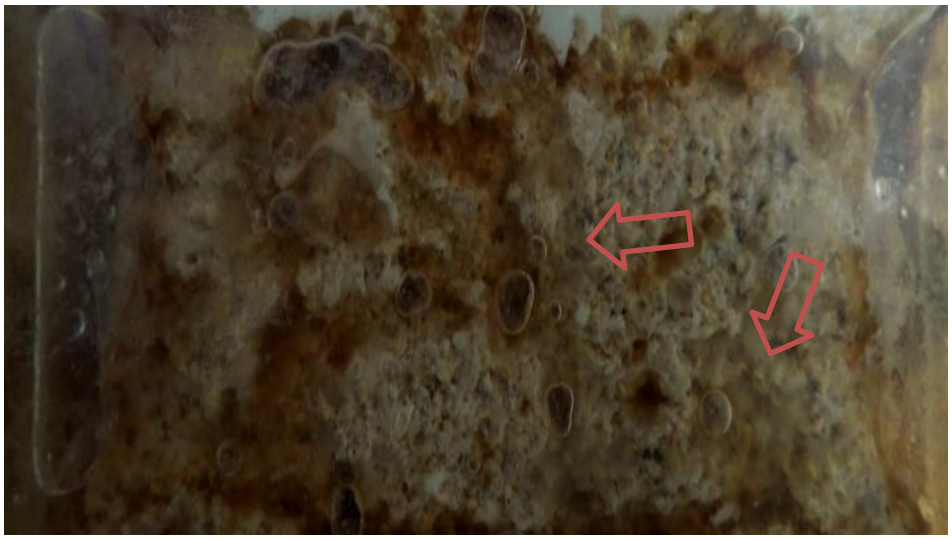

Figure 7.30- Top view after 90 minutes of injection of distilled water at a rate of 0.05 ml/min.

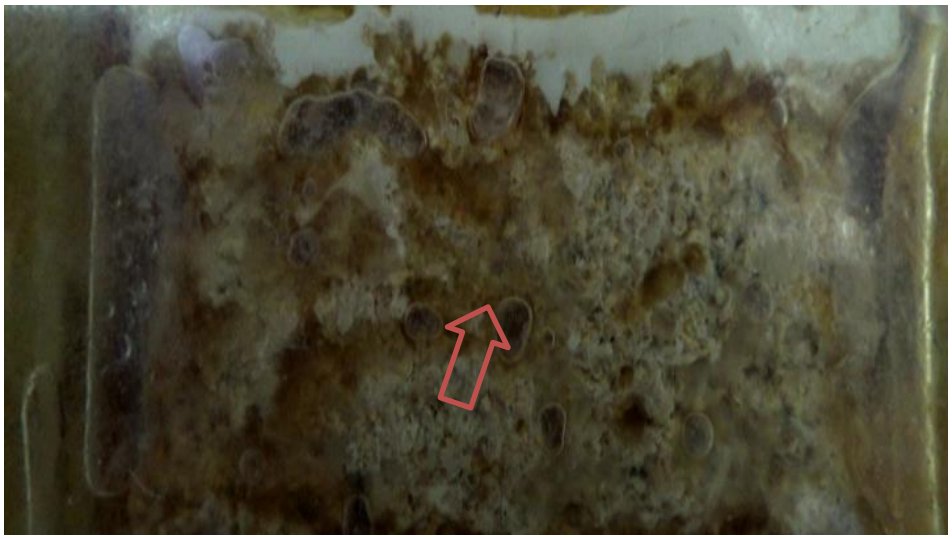

Figure 7.31- Top view after 3 hours of injection of distilled water at a rate of 0.05 ml/min.

Figure 7.32- Top view after 5 hours of injection of distilled water at a rate of 0.05 ml/min.

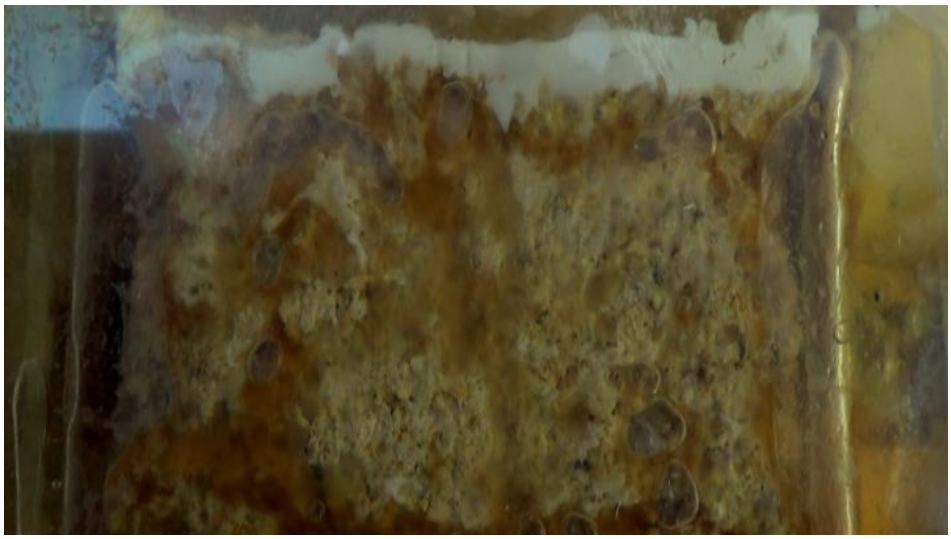

Figure 7.33- Top view before injection of liquid detergent solution.

Figure 7.34- Top view after 30 minutes of injection of liquid detergent solution at a rate of 0.05 ml/min.

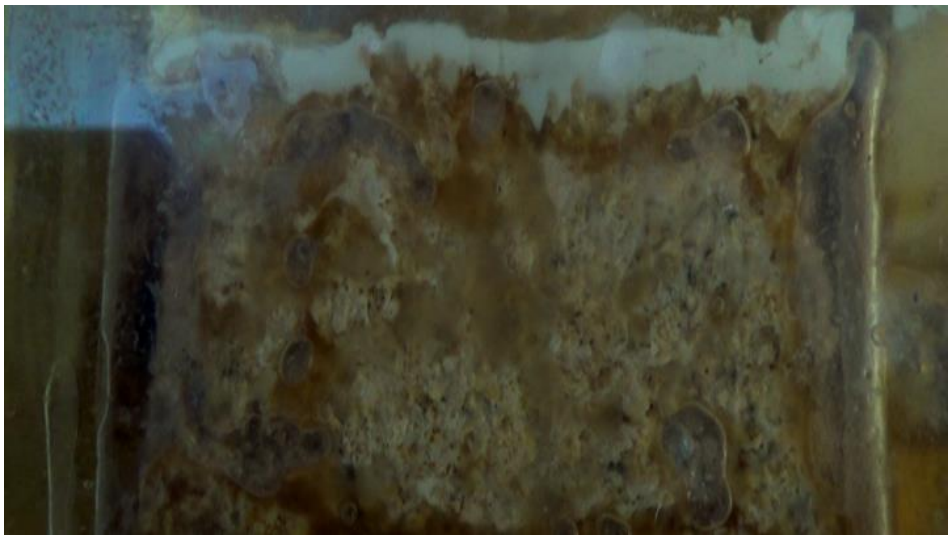

Figure 7.35- Top view after 60 minutes of injection of liquid detergent solution at a rate of 0.05 ml/min.

Figure 7.36- Top view after 90 minutes of injection of liquid detergent solution at a rate of 0.05 ml/min.

Figure 7.37- Top view after 3 hours of injection of liquid detergent solution at a rate of 0.05 ml/min.

CHAPTER 8

APPLICATION OF X-RAY COMPUTERIZED TOMOGRAPHY

8.1 Materials

The core sample is a highly permeable limestone which includes small amounts of quartz and feldspar apart from the calcite mineral. Petrography analysis did not indicate any fractures and water soluble components in the sample.

The diameter and length of the core sample were measured as 3.53 cm and 9.85 cm, respectively.

200 g/L NaCl solution and toluene were used to saturate the core sample. The NaCl solution, sulfated brine, SW*4SO_4 (Figure 4.2) and liquid detergent solution were injected to recover oil.

The NaCl solution was selected to avoid $CaSO_4$ precipitation during sulfated brine injecion. The brine, SW*4SO_4 was selected as an injecting liquid to recover oil as the highest water wet fractions were commonly obtained using this liquid in wettability measurements. Liquid detergent composed of % 5 – 15 anionic surfactant, <% 5 nonionic surfactant and preservatives which are benzisothiazolione, phenoxyethanol and geraniol was tested at the final step after sulfated brine injection to see if any further improvement in oil recovery can be achieved reducing the interfacial tension.

X-ray computerized tomography (CT) was applied to observe changes inside the core sample after injection of each liquid. Brand name of the device is Hitachi and the model is Radix Turbo.

8.2 Core Preparation

Lateral face of the core sample was wrapped with epoxy. Inlet and outlet sections were closed with teflon lids to which connectors were attached. O rings were placed between the teflon lids and core sample in order to prevent leakage of the injected liquid and to provide some space at the inlet and outlet of the sample. The teflon lids were connected with screws (Figure 8.1).

Figure 8.1- View of the core sample used in the tomography application.

Two displacement runs were carried out to compare the effectiveness of high saline formation water and sulfate rich brine on oil recovery. The core was prepared with the following procedure for both experiments:

- Initially, the core was saturated with 200 g/L NaCl solution (high saline brine) under evacuation.

- After being aged in the brine sample for 7 days, the sample was saturated with toluene. Toluene was injected at a rate of 13 ml/min for 3 pore volume in one direction and for 1 pore volume in the reverse direction.

- The core sample was aged in toluene for 5 days before injection of the brine samples for oil recovery.

Porosity was determined as 0.51 as fraction from the weight difference between dry and wet core. In both experiments, total water production was measured as nearly 23 ml after injection of 3 pore volume toluene and production of water was not observed during injecting in the reverse direction. Oil saturation was calculated as 0.47 as fraction for both experiments dividing the produced water volume (23 ml) to pore volume which is 49.2 ml.

8.3 Procedure

In the first experiment, the following steps were applied in sequence for oil production:

- High saline brine used to saturate the core sample was injected until production of toluene was not observed. After injection of high saline brine, CT was applied.

- Sulfated brine, SW*4SO_4 was injected for around 3 pore volumes. After injection of the sulfated brine, CT was applied.

- Sulfated brine, SW*4SO_4 was injected again after 1 day of aging in this brine sample. After injection of the sulfated brine, CT was applied.

- Sulfated brine, SW*4SO_4 was injected again after 3 days of aging in this brine sample. After injection of the sulfated brine, CT was applied.

After the first experiment was conducted, the core sample was flooded with 9 pore volume of distilled water and was dried in the oven to prepare it for the second experiment.

In the second experiment, the following steps were applied in sequence for oil production:

- Sulfated brine, SW*4SO_4, was injected directly not performing the high saline brine injection priorly. The injection process continued until production of toluene was not observed. After injection of the sulfated brine, CT was applied.

- 0.5 g/L liquid detergent solution was injected for around 6 pore volumes. After the injection process, CT was applied.

The injection rate was kept constant at 1 ml/min both in the first and second experiments.

Table 8.1 shows the parameters associated to the CT measurements. X-ray generator produced electric current of 175 milli ampere close to maximum value (200 milli ampere) that the machine can produce. The spot size was taken equal to the slice thickness during the measurements. Figure 8.2 shows the illustration of the spot size, slice thickness and sections on the view from top of the core sample.

Table 8.1- Parameters associated to measurements conducted using X-ray tomography.

Spot Size (mm)	**Scan Time (second)**	**Electric Current (mA)**	**Voltage (kV)**	**Matrix**	**Slice Thickness (mm)**
2, 5	1	175	120	512	2, 5

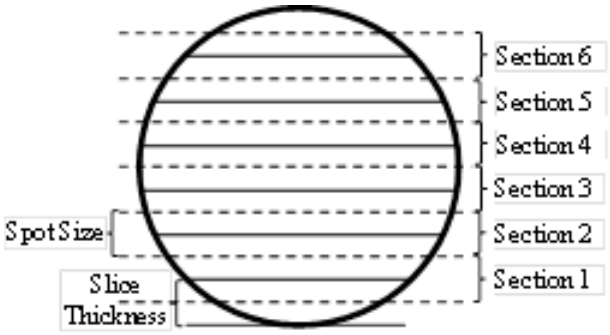

Figure 8.2- Illustration of the spot size, slice thickness and sections on the top view of the core sample.

8.4 Results and Discussion

Figure 8.3 and Figure 8.4 show the average values of the CT readings at 0.5 cm wide sections taken along the diameter of the core sample in vertical direction. The following abbreviations are used for the cases:

- HBTS1: The case in which the sample was saturated with high saline brine and toluene in the first experiment.

- HBTS2: The case in which the sample was saturated with high saline brine and toluene in the second experiment.

- HBS: The case in which the sample was fully saturated with high saline brine.

- ATS: The case after the sample was saturated with toluene.

- BHB: The case before high saline brine injection for oil recovery after 5 days of aging process in the first experiment.

- AHB: The case after high saline brine injection in the first experiment.

Existence of slight differences between the average values belonging to first and second experiments in Figure 8.3 indicates that the core sample was saturated with

nearly same amounts of toluene in the first and second experiments, the fact which was also confirmed with produced amounts. Decrease in CT values as a result of displacing the brine with toluene and increase in the values as a result of production of toluene are both observable in Figure 8.4.

Table 8.2 shows the multiplications of porosity and oil saturation calculated using the average CT values shown in Figure 8.3 and Figure 8.4. The multiplications were obtained dividing the difference between CT values for fully brine saturated core and for brine and toluene saturated cores to the difference between CT values for the brine, 598 and for toluene, -193. The multiplications belonging to HBTS1, BHB and HBTS2 are all close to each other and consistent with the measured values.

$$\Phi S_o = (A-B)/(C-D) \quad (8.1)$$

A: CT value for fully brine saturated core.

B: CT value for brine and toluene saturated core.

C: CT value for the brine, 598.

D: CT value for toluene, -193.

Figure 8.5 shows the recovery with respect to injected pore volumes. Injection of $SW*4SO_4$ did not result in any improvement in recovery after high saline brine injection in the first experiment. Aging process was also not beneficial. The situation was different in the second experiment including direct injection sulfated brine without performing high saline brine injection. The recovery reached to 45 % of OIP more than the ultimate recovery obtained injecting high saline brine. Utilizing liquid detergent afterwards was not beneficial in improving the recovery.

Figures 8.6 and 8.7 belonging to the first experiment show CT values in color when the core sample was dry, after the core sample was saturated with high saline brine, after injection of toluene, before high saline brine injection after 5 days of aging period, after high saline brine injection and after sulfated brine injection at the sections having thickness of 2 mm.

The color changes from blue to green, from green to yellow, from yellow to red and from red to black as CT value gets higher. The core sample was indicated with green to blue, yellow, red and black colors in the middle of the figures. The region in light blue color near the section showing the sample indicates the epoxy wrapping the core sample and the thin region in yellow color near the region showing the sample indicates cement used to prevent the leakage of the epoxy into the sample as it hardened. Other parts having a dark blue color indicate the air zone.

Alteration in color in the region indicating the core sample was due to the differentiation in porosity. The difference is more pronounced in the figures belonging to the case in which the core sample was dry. The sections shown with blue to green color have higher porosity than the porosity of the sections indicated with yellow and red colors.

Increase in CT values after saturating the core sample with brine and decrease in CT values after injecting toluene can be observable in the figures. The changes occurred after production of toluene might not be noticeable in the figures, but the increase is clear in Figure 8.4. It is seen from the figures that 5 days of aging period did not result in significant changes in the distribution of the liquids inside the core sample. Increase in CT values are observable in some regions indicated with ovals in the figures belonging to the case before high saline brine injection after 5 days of aging period, which might be an indication of replacement of toluene with the brine sample as the CT value of the brine sample is higher than the CT value of toluene. Injection of sulfated brine being less dense than NaCl solution brought decrease in CT values.

Difference between the cases before high saline brine injection and after sulfated brine injection in the first experiment is that 8.5 ml of produced toluene was replaced with sulfated brine and around 26 ml of high saline brine taking place inside the core sample before high saline brine injection was replaced with sulfated brine. Replacement of toluene with sulfated brine brought increase in CT values as the CT value for the sulfated brine, 40 is higher than the CT value for the toluene -193. On

the other hand, replacement of high saline brine with sulfated brine caused decrease in CT values as the CT value for high saline brine, 598 is higher than the CT value for the sulfated brine. It can be deduced from the related figures that CT values obtained after sulfated brine injection is commonly less than the CT values obtained before high saline brine injection. Decrease in CT values as a result of displacement of high saline brine with sulfated brine is much more than the increase which is as a result of replacement of toluene with sulfated brine since displacement of high saline brine occurred in a larger volume and the difference between the CT values of the liquids is higher in that case.

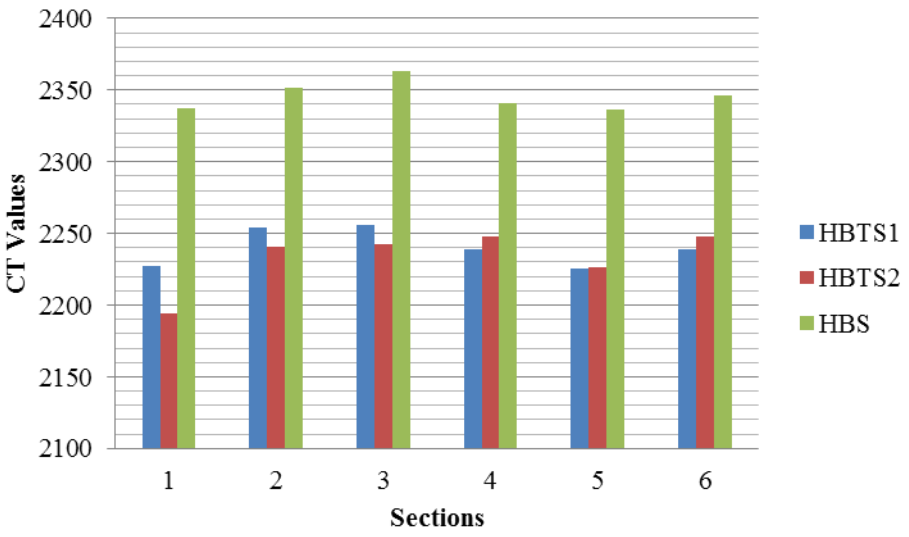

Figure 8.3- CT values at differet sections for the cases in which the sample was saturated with high saline brine and toluene in the first and second experiments (HBTS1, HBTS2) and the sample was fully saturated with high saline brine (HBS).

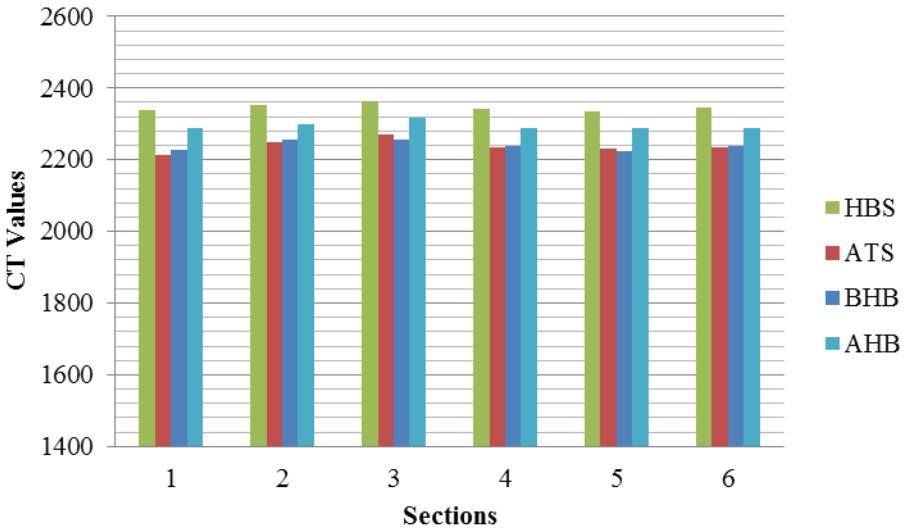

Figure 8.4- CT values at different sections for the cases in which the sample was fully saturated with high saline brine (HBS), after the sample was saturated with toluene (ATS) and before high saline brine injection (BHB).

Table 8.2- Multiplications of porosity and oil saturation for the cases in which the sample was saturated with high saline brine and toluene in the first and second part of the experiment (HBTS1, HBTS2) and before and after high saline brine injection (BHB, AHB).

Section/ ϕ*So (%)	HBTS1	BHB	HBTS2	AHB
1	27.22	24.33	31.66	11.10
2	22.36	21.54	24.69	11.70
3	20.27	23.88	26.75	10.08
4	23.28	22.71	20.77	11.47
5	23.33	24.60	24.46	10.73
6	24.54	23.73	21.66	12.61
Average:	22.76	23.29	23.67	11.32

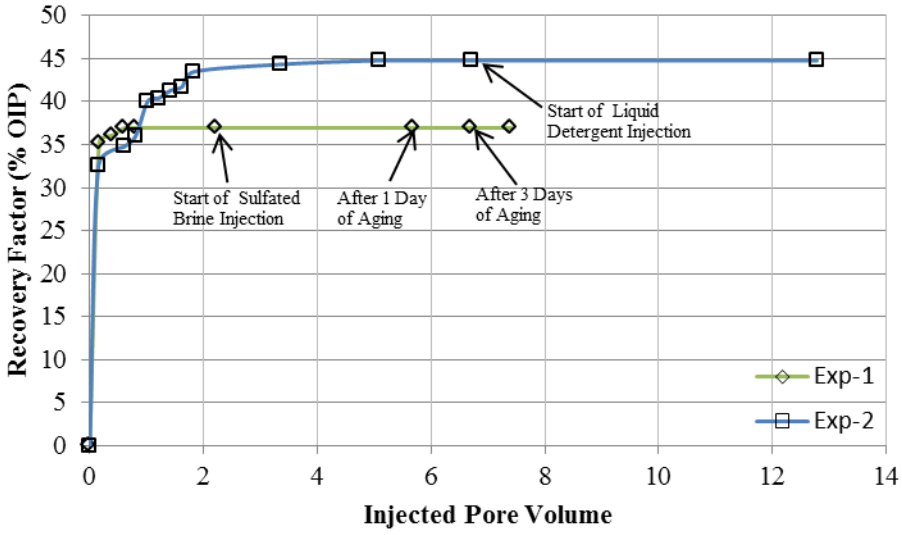

Figure 8.5- Recovery factor with respect to injected pore volume.

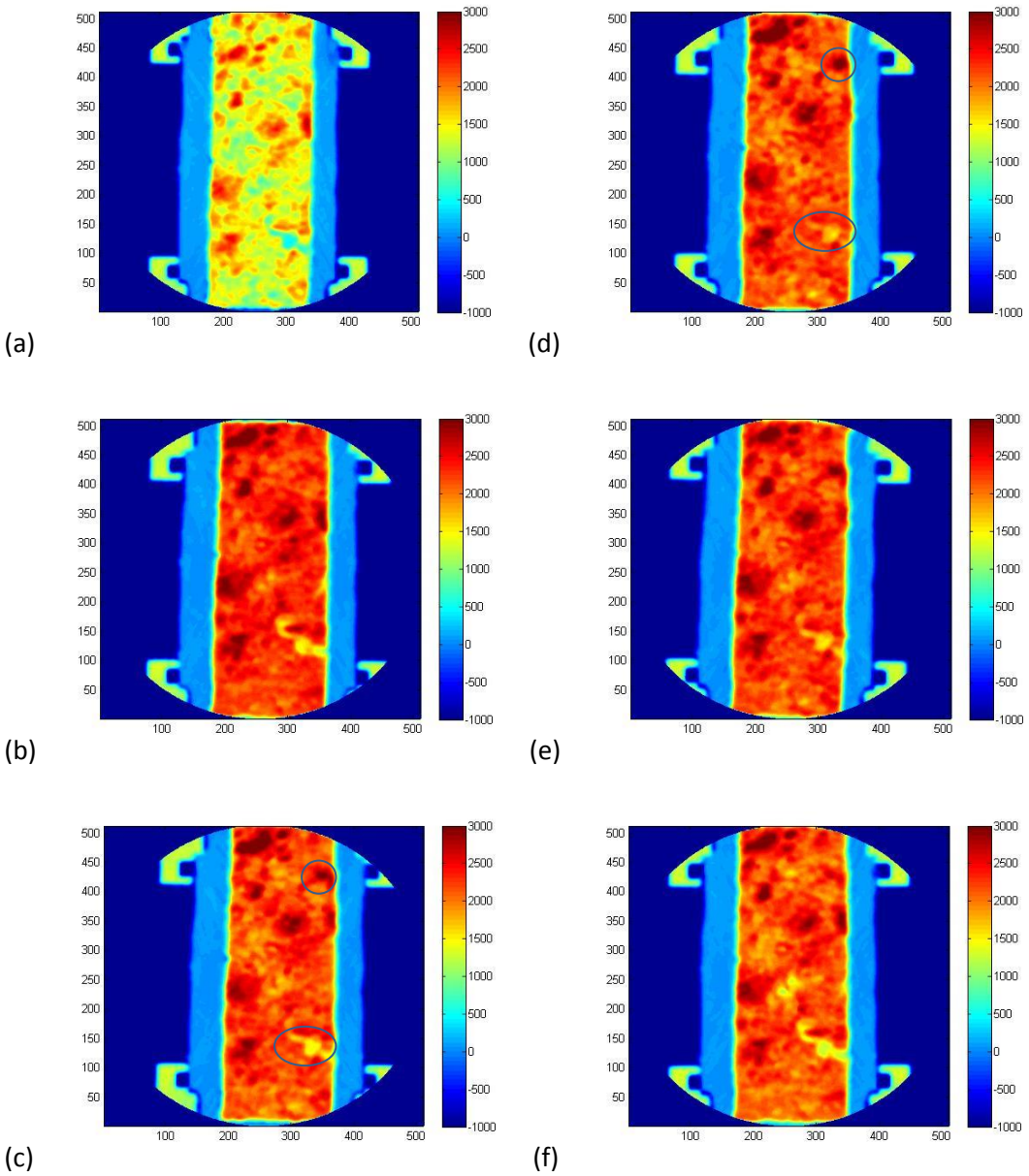

Figure 8.6- CT readings for the dry core (a), water saturated core (b), water and toluene saturated core (S_w = % 53) (c), before high saline brine injection (d), after high saline brine injection (e) and after sulfated brine injection (f) at L = 1.0 cm.

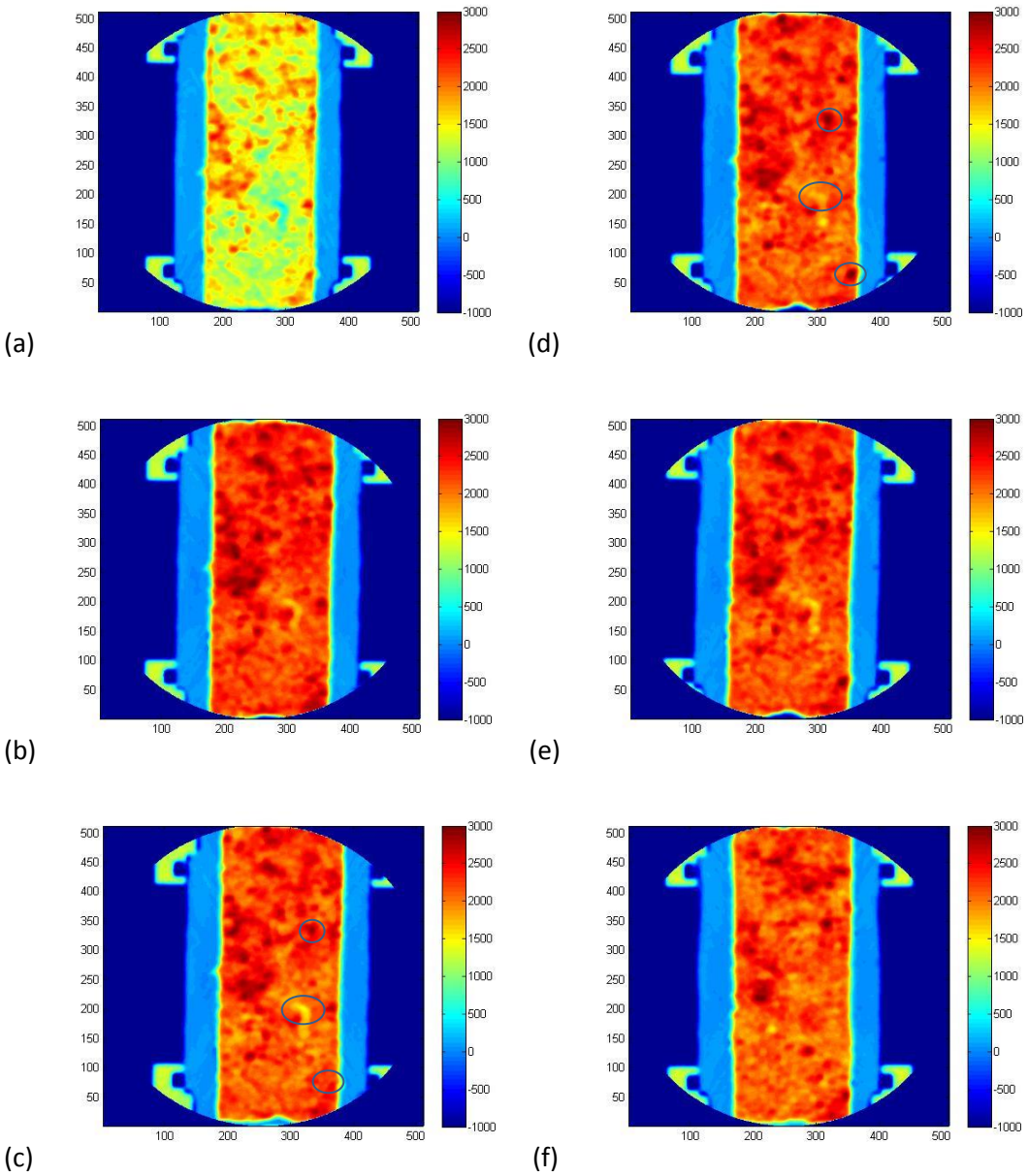

Figure 8.7- CT readings for the dry core (a), water saturated core (b), water and toluene saturated core (S_w = % 53) (c), before high saline brine injection (d), after high saline brine injection (e) and after sulfated brine injection (f) at L = 2.0 cm.

CHAPTER 9

CONCLUSIONS

The following conclusions were drawn from this study:

Sulfate ions become more effective in increasing water wettability of carbonates when they are used in conjunction with divalent cations.

Sandstone samples interacting with divalent cations can be more oil-wet compared to the samples interacting with sodium ions. Utilization of low saline brine might not be helpful in increasing water wettability of sandstone samples being poor in clay content.

High water wettability can be attained for carbonates even at low temperatures increasing the sulfate concentration in the low saline brine.

The sodium ion becomes more effective in increasing the sulfated brine wettability for carbonates as the polarity of the oil phase decreases.

The compound $MgSO_4$ is not effective in increasing the water wettability for carbonates at low temperatures because of the formation of strong ion pairs. High temperatures are needed for the dissociation of the ions.

Improvement in spontaneous imbibition of brines into carbonates can be achieved decreasing the interfacial tension between oil and brine by means of using surfactants or decreasing the salinity.

Core flooding studies indicated that low saline sulfated brines could be more effective than formation brine samples in recovering the oil from carbonates. It was

observed that direct utilization of sulfated brine including divalent cations not injecting of high saline brine used to saturate the core sample previously led to more oil production.

Spontaneous imbibition of water from fractures into matrix can be achieved using smart water as a wettability modifier for neutral wet to oil wet reservoirs. Increase in water wettability with smart water utilization will lower the energy requirement to displace oil in the reservoir. Possible decrease in interfacial tension between oil and water with decrease in salinity can result in a contribution as the salinity of the smart waters is much lower than the salinity of typical formation brines. The success of the process depends on numerous factors related to liquid and rock properties and also on temperature.

REFERENCES

1. Yousef, A.A., Al-Saleh, S., Al-Jawfi, M., "New Recovery Method for Carbonate Reservoirs through Tuning the Injection Water Salinity: Smart WaterFlooding", Paper SPE 143550, 2011.

2. University of Stavanger, "Smart Water in Carbonates", http://www.uis.no/research-and-phd-studies/research-areas/oil-gas-and-renewable-energy/petroleum-engineering/reservoir-engineering/research-activities/water-based-eor-from-carbonates-and-sandstones-by-smart-water/smart-water-in-carbonates/, last visited on October 2015, 2013.

3. University of Stavanger, "Smart Water in Sandstone", http://www.uis.no/research-and-phd-studies/research-areas/oil-gas-and-renewable-energy/petroleum-engineering/reservoir-engineering/research-activities/water-based-eor-from-carbonates-and-sandstones-by-smart-water/smart-water-in-sandstone/, last visited on October 2015, 2013.

4. Hognesen, E.J., Strand, S., Austad, T., "'Waterflooding of Prefential Oil-Wet Carbonates: Oil Recovery Related to Reservoir Temperature and Brine Composition", Paper SPE 94166, 2005.

5. Zhang, P., Austad, P., "Wettability and Oil Recovery from Carbonates: Effects of Temperature and Potential Determining Ions", Elsevier, Volume 279, Issues 1-3, 15 May 2006, Pages 179-187.

6. Anderson, W.G., "Wettability Literature Survey – Part 6: The Effects of Wettability on Waterflooding", Paper SPE, 1987.

7. Anderson, W.G., “Wettability Literature Survey – Part 4: The Effects of Wettability on Capillary Pressure”, Paper SPE, 1987.

8. Anderson, W.G., “Wettability Literature Survey – Part 5: The Effects of Wettability on Relative Permeability”, Paper SPE, 1987.

9. Brock, D.C., Orr, F.M., “Flow Visualization of Viscous Fingering in Heterogeneous Porous Media”, Paper SPE 22614, 1991.

10. Romanuka, J., Hofman, J.P., Ligthelm, D.J., Suijkerbuijk, B.M.J.M., Marcelis, A.H.M., Oedai, S., Brussee, N.J., Linder, H.A., Aksulu, H., Austad, T., “Low Salinity EOR in Carbonates”, Paper SPE 153869, 2012.

11. Martavaltzi, C., Dakik, A., Agrawal, S., Gupta, A., “Wettability Alteration of Carbonates by Optimizing the Brine and Surfactant Composition”, Paper SPE 163348, 2012.

12. Kathel, P., Mohanty, K.K., “EOR in Tight Oil Reservoirs through Wettability Alteration”, Paper SPE 166281, 2013.

13. Seethepalli, A., Adibhatla, B., Mohanty, K.K., “Wettability Alteration During Surfactant Flooding of Carbonate Reservoirs”, Paper SPE 89423, 2004.

14. Hamouda, A.A., Gomari, K.A.R., “Influence of Temperature on Wettability Alteration of Carbonate Reservoirs”, Paper SPE 99848, 2006.

15. Al-Hadhrami, H.S., “Thermally Induced Wettability Alteration to Improve Oil Recovery in Fractured Reservoirs”, Paper SPE 59289, 2000.

16. Roosta, A., Escrochi, M., Varzandeh, F., Khatibi, J., Ayatollahi, S., Schafiee, M., “Investigating the Mechanism of Thermally Induced Wettability Alteration”, Paper SPE 120354, 2009.

17. Shidong, L., Torsaeter, O., “The Impact of Nanoparticles Adsorption and Transport on Wettability Alteration of Intermediate Wet Berea Sandstone”, Paper SPE 172943, 2015.

18. Puntervold, T., Austad, T., “Injection of Seawater and Mixtures with Produced Water into North Sea Chalk Formation: Impact on wettability, scale formation and rock mechanics caused by fluid-rock interaction”, Paper SPE 111237, 2007.

19. Fathi, S.J., Austad, T., Strand, S., “Smart Water as Wettability Modifier in Chalk: The Effect of Salinity and Ionic Composition”, Energy & Fuels 2010, 24, 2514-2519.

20. Strand, S., Austad, T., Puntervold, T., Hognesen, E.J., Olsen, M., Barstad S.M., “Smart Water for oil Recovery from Fractured Limestone: A preliminary Study”, Energy & Fuels 2008, 22, 3126-3133.

21. Korsnes, R.I., Madland, M.V., Austad, T., Haver, S., Rosland, G., “The Effects of Temperature on the Water Weakening of Chalk by Seawater”, Paper Society of Core Analysts (SCA) 2006-37.

22. Alotaibi, M.B., Nasralla, R.A., Nasr-El-Din, H.A., “Wettability Challenges in Carbonate Reservoirs”, Paper SPE 129972, 2010.

23. Gupta, R., Smith, P.G., Willingham, T.W., Lo Cascio, M., Shyeh, J.J., Harris, C.R., "Enhanced Waterflood for Middle East Carbonate Cores-Impact of Injection Water Composition", Paper SPE 142668, 2011.

24. Austad, T., RezaiDoust, A., Puntervold, T., "Chemical Mechanism of Low Salinity Waterflooding in Sandstone reservoirs", Paper SPE 129767, 2010.

25. RezaiDoust, A., Puntervold, T., Strand, S., Austad, T., "Smart Water as Wettability Modifier in Carbonate and Sandstone: A Discussion of Similarities/Differences in the Chemical Mechanics", Energy & Fuels, 2009, 23, 4479-4485.

26. Wang, W., Gupta, A., "Investigation of the Effect of Temperature and Pressure on Wettability Using Modified Pendant Drop Method", Paper SPE 30544, 1995.

27. Austad, T., RezaiDoust, A., Puntervold, T., "Chemical Mechanism of Low Salinity Waterflooding in Sandstone reservoirs", Paper SPE 129767, 2010.

28. Gerald, S., "Electric Double Layer", http://web.nmsu.edu/~snsm/classes/chem435/Lab14/double_layer.html, last visited on December 2014, 2011.

29. Rahbar, M., Ayatollahi, S., Ghatee, M.H., "The Roles of Nano-Scale Intermolecular Forces on the Film Stability During Wettability Alteration Process of the Oil Reservoir Rocks", Paper SPE 132616, 2010.

30. Buckley, J.S., Liu, Y., Monsterleet, S., "Mechanisms of Wetting Alteration by Crude Oils", Paper SPE 37230, 1998.

31. Anderson, W.G., “Wettability Literature Survey-Part 1: Rock/Oil/Brine Interactions and the Effects of Core Handling on Wettability”, Paper SPE 13932, 1986.

32. Wolcott, J.M., Groves, F., Lee H.G., “The Influence of Crude Oil Composition on Mineral Adsorption and Wettability”, Paper SPE 25194, 1996.

33. Al-Maamari, R.S.H., Buckley, S.B., “Asphaltene Precipitation and Alteration of Wetting: Can Wettability Change during Oil Production”, Paper SPE 59292, 2000.

34. Escrochi, M., Nabipour, M., Ayatollahi, Sh., Menranbod, N., “Wettability Alteration at Elevated Temperatures: The Consequences of Asphaltene Precipitation”, Paper SPE 112428, 2008.

35. Appleyard, S.P., Cope, D.P., Gharfeh, S.G., Singh, P., “Prediction of Asphaltene Stability for Live Oils – Impact of Changes in Temperature, Pressure and Composition”, International Petroleum Technology Conference (IPTC) 13650, 2009.

36. Skauge, A., Standal, S., Boe, S.O., Skauge, T., Blokhus, A.M., “Effects of Organic Acids and Bases and Oil Composition on Wettability”, Paper SPE 56673, 1999.

37. Kim, S.T., Bound-Hir, M.E., Mansoori, G.A., “The Role of Asphaltene in Wettability Reversal”, Paper SPE 20700, 1990.

38. Hematfar, V., Maini, B.B., Chen, Z., “Influence of Clay Minerals and Water Film Properties on In-Situ Adsorption of Asphaltene”, Paper SPE 165506, 2013.

39. Zhang, P., Austad, T., "The Relative Effects of Acid Number and Temperature on Chalk Wettability", Paper SPE 92999.

40. Alotaibi, M.B., Nasralla, R.A., Nasr-El-Din, H.A., "Wettability Studies Using Low-Salinity Water in Sandstone Reservoirs", Paper SPE 149942, 2011.

41. Aveyard, R., Saleem, S.M. 1976. "Interfacial Tensions at Alkane-Aqueous Electrolyte Interfaces", Journal of the Chemical Society, Faraday Transactions *1(72):* 1609–1617.

42. Cai, B., Yang, J., Guo,T., "Interfacial Tension of Hydrocarbon+Water/Brine Systems under High Pressure", Journal of Chemical and Engineering Data 41(3), 1996.

43. Serrano-Saldaña, E. et al., "Wettability of Solid/Brine/N-dodecane Systems: Experimental Study of the Effects of Ionic Strength and Surfactant Concentration", Colloids and Surfaces A: Physicochemical and Engineering Aspects 241(1–3), 2004.

44. Hamouda, A.A., Karoussi, O., "Effect of Temperature, Wettability and Relative Permeability on Oil Recovery from Oil-wet Chalk", Energies 1, 2008.

45. Okasha, T.M., Al-Shiwaish, A.A., "Effect of Brine Salinity on Interfacial Tension in Arab-D Carbonate Reservoir, Saudi Arabia", Paper SPE 119600, 2009.

46. Isehunwa, S.O., Olubukola, O., "Interfacial Tension of Crude Oil-Brine Systems in the Niger Delta", IJRRAS 10 (3), 2012.

47. Vijapurapu, C.S., Rao, D.N., “Compositional Effects of Fluids on Spreading, Adhesion and Wettability in Porous Media”, Colloids and Surfaces. A: Physicochemical and Engineering Aspects 241 (1–3), 2004.

48. Jennings, H.Y., “The Effect of Temperature and Pressure on the Interfacial Tension of Benzene-Water and Normal Decane-Water”, Journal of Colloid and Interface Science 24 (3), 1967.

49. McCaffery, F.G., “Measurement of Interfacial Tension and Contact Angles at High Temperature and Pressure”, Journal of Canadian Petroleum 11, 1972.

50. Hjelmeland, O.S., Larrondo, L.E., “Experimental Investigation of the Effects of Temperature, Pressure, and Crude Oil Composition on Interfacial Properties”, SPE Reservoir Engineering 1 (4), 1986.

51. Strand, S., Hognesen, E.J., Austad, T., “Wettability Alteration of Carbonates – Effects of Potential Determining ions (Ca^{2+} and SO_4^{2-}) and Temperature”, Colloids and Surfaces A: Physicochemical and Engineering Aspects, 275 (1-10), 2006.

52. Nasralla, R.A., Nasr-El-Din, H.A., “Impact of Electrical Surface Charges and Cation Exchange on Oil Recovery by Low Salinity Water”, Paper SPE 147937, 2011.

53. Hiorth, A., Cathles, L.M., Madland, M.V., “The Impact of Pore Water Chemistry on Carbonate Surface Charge and Oil Wettability”, Transp Porous Med 85, 2010.

54. Mwangi, P., Thyne, G., Rao, D., “Extensive Experimental Wettability Study in Sandstones and Carbonate Oil-Brine Systems: Part 1 – Screening Tool Development”, Paper Society of Core Analysts (SCA), 2013-84.

55. Osgouei, Y.T., “An Experimantal Study on Steam Distillation of Heavy Oils during Thermal Recovery”, M.S. Thesis, Middle East Technical University, February 2013.

56. Khan, M.T., Zeytçioğlu, M., Saner, S., “Micro Scale Sweep Visualization Experiments Using Carbonate Samples”, Earthdoc, 2013.

CURRICULUM VITAE

PERSONAL INFORMATION

Surname, Name: Polat, Can

Nationality: Turkish (TC)

Date and Place of Birth: 17 April 1984, Edirne

Marital Status: Single

Email: pcan@metu.edu.tr

EDUCATION

Degree	Institution	Year of Graduation
MS	METU Petroleum and Natural Gas Engineering	2010
BS	METU Petroleum and Natural Gas Engineering	2007
High School	Hacı Ömer Tarman Anadolu High School, Ankara	2002

WORK EXPERIENCE

Year	Place	Enrollment
2007-2015	METU Department of Petroleum and Natural Gas Engineering	Research Assistant